Journal Pre-proof

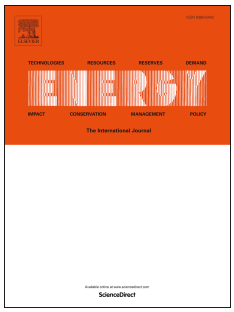

Investigation into ethanol effects on combustion and particle number emissions in a spark-ignition to compression-ignition (SICI) engine

Qinhao Fan, Shang Liu, Yunliang Qi, Kaiyuan Cai, Zhi Wang

PII: S0360-5442(21)01418-3

DOI: https://doi.org/10.1016/j.energy.2021.121170

Reference: EGY 121170

To appear in: *Energy*

Received Date: 1 February 2021

Revised Date: 22 May 2021

Accepted Date: 2 June 2021

Please cite this article as: Fan Q, Liu S, Qi Y, Cai K, Wang Z, Investigation into ethanol effects on combustion and particle number emissions in a spark-ignition to compression-ignition (SICI) engine, *Energy*, https://doi.org/10.1016/j.energy.2021.121170.

Credit Author Statement

Qinhao Fan: Conceptualization, Methodology, Investigation, Data curation, Writing - Original Draft. Shang Liu: Investigation, Formal analysis. Yunliang Qi: Methodology, Writing - Review & Editing, Project administration. Kaiyuan Cai: Investigation, Resources. Zhi Wang: Supervision, Project administration, Funding acquisition

Investigation into ethanol effects on combustion and particle number emissions in a spark-ignition to compression-ignition (SICI) engine

Qinhao Fan[a], Shang Liu[a], Yunliang Qi [a*, b], Kaiyuan Cai[a], Zhi Wang[a]

[a] State Key Laboratory of Automotive Safety and Energy, Tsinghua University, Beijing 100084, China

[b] Graduate Aerospace Laboratories, California Institute of Technology, Pasadena, CA 91125, USA

*Corresponding author: Yunliang, Qi

Graduate Aerospace Laboratories, California Institute of Technology

Pasadena, 91125, USA

Email: qiyl@caltech.edu

Abstract

Spark assistance along with oxygenated components addition is a promising method to achieve stable compression ignition, high thermal efficiency and low particle emission. To this end, ethanol blended with non-oxygenated gasoline was fueled to an engine working with spark-ignition to compression-ignition (SICI) mode under air dilution and exhaust-diluted conditions. The effects of ethanol addition on engine performance including combustion characteristics, fuel economy, particle number (PN) emissions, were studied in two categories: changing research octane number (RON) by varying ethanol content and maintaining RON by changing fuel type. The results showed that ethanol addition by splash blending suppressed knock tendency, and the knock intensity could be lowered by up to 65~75% with increasing ethanol content. However, when maintaining the same RON, the ethanol-gasoline blend exhibited higher knock intensity than pure gasoline due to

synergistic effects between ethanol and aromatics on auto-ignition. Compared to pure spark ignition with high-RON gasolines, using ethanol-gasoline blends under SICI could reduce the minimum fuel consumption rate by up to 25 g/(kW·h). To characterize the high-efficiency cycles under SICI, two dimensionless parameters were proposed by considering the ratios of heat release amount and duration between the flame propagation stage and auto-ignition stage. The two parameters showed good exponential correlation. As for emissions, blending ethanol could basically reduce PN emissions under SICI mode except for the cases with significant increase in nucleation particles, such as those with high knock intensity under stoichiometric condition and poor combustion quality under heavily exhaust-diluted conditions. The total PN reduction by blending ethanol is mainly due to the decrease of accumulation mode particles, during the stage of flame propagation rather than auto-ignition. Blending ethanol into non-oxygenated gasoline will directly increase unburned hydrocarbons and nitrogen oxides due to the low auto-ignition propensity of ethanol under stoichiometric or moderately lean conditions according to the temperature-pressure trajectory. Therefore, a dedicated combustion system with higher compression ratio and lean-boosted mixture is required to enhance ethanol's reactivity and achieve better fuel economy along with low PN emission for diluted SICI combustion.

Keyword

Spark-ignition to compression-ignition; Ethanol blends; Fuel economy; Particle number emission; Fuel reactivity

1. Introduction

Spark assistance is an effective method to improve combustion stability and extend engine load of homogeneous charge compression ignition (HCCI) [1-6], which has been applied in Mazda

SKYACTIV-X [7] and can be further combined with vehicle electrification in near future. From the viewpoint of transportation energy, blending oxygenated components with conventional hydrocarbon fuels is beneficial to green-house gas (GHG) and particulate emission reduction while co-optimization of engines and oxygenated fuel is required [8]. Among oxygenated components, ethanol has been widely used both in spark ignition (SI) engines [9, 10] and compression ignition (CI) engines [11, 12]. Due to the high research octane number (RON) and octane sensitivity (S), ethanol can enhance knock resistance in "beyond RON" regions [13, 14], suitable for SI engines with high compression ratios (CRs). In addition, with higher laminar flame speed and smaller molecular weight compared with gasoline and diesel, ethanol improves local oxidation and decreases activation energy of soot oxidation [15], conducive to particle matter reduction [12, 16] both under SI and CI modes.

In order to further extend knock/lean limit and improve thermal efficiency, several methods, including fuel stratification [17-19], hydrogen-alcohols dual-fuel strategy [20-23] and high-energy spark assistance [7, 24], have been used in engines fueling low-carbon alcohols. Han et al. [18] compared the influence of injection timing (intake or compression stroke) and number of injections on fuel consumption and emissions using research-grade E10 gasoline. The results showed that the injection timing had more significant influence than the number of injection on knock resistance and gaseous emission reduction because of stratification and charge cooling effect. Wang et al. [20] and Liu et al. [21] studied alcohols-gasoline and gasoline-alcohols dual-fuel mode in SI engines and also found that direct injection of alcohol could better utilize the latent heat of vaporization to mitigate engine knock. To achieve better combustion control and extend operation boundary of steady combustion, Gong et al. [22, 23] used methanol and hydrogen for ultra-lean burn. They demonstrated that the engine could operate steadily with hydrogen-enriched methanol at excess air ratio of 2.95,

and the combustion center could still be maintained within 10 °CA ATDC. Moreover, a slight hydrogen addition (6%) could lower hydrocarbons emission much compared with pure methanol. Among the aforementioned methods, spark assistance along with fuel stratification has a relatively low cost and only requires one fuel supply system, which has the potential to be applied in the combustion modes involving controlled auto-ignition, such as spark-ignition to compression-ignition (SICI) mode, in the near future.

SICI combustion has been substantially studied in engines and fundamental research devices, e.g., rapid compression machines (RCM), using pure high-RON gasolines [1-6, 26-29], ethanol-gasoline blends [24, 31] and their surrogate fuels [32-37] in the past decade. Specifically, Wang et al. [1] achieved SICI combustion at medium–high loads using commercial 93# gasoline and external exhaust gas recirculation (EGR), an indicated specific fuel consumption (ISFC) less than 225 g/kW·h was obtained at about 22% EGR. Olesky et al. [3, 5, 26] investigated the influence of intake temperature, spark advance for flame limit extension and diluent composition on heat release ratio rate using RON 87 gasoline provided by Chevron Phillips. The results showed that the advanced spark timing could compensate for the decrease in intake temperature. The moderately advanced spark timing could enhance combustion robustness, but too early spark timing could hardly adjust combustion phasing. The duration of auto-ignition portion was relatively insensitive to diluent composition compared to the deflagration (flame propagation) portion, because the auto-ignition portion has a faster heat release controlled by chemical kinetics rather than thermo-mass diffusion. Moreover, positive valve overlap (PVO) and negative valve overlap (NVO) were also used in SICI combustion to extend engine load and elevate thermodynamic states at the top dead center (TDC), respectively. Xie et al. [2] systematically proposed an optimized PVO and external EGR strategy in

the range of 0.5-0.9 MPa IMEP (Indicated mean effective pressure) using RON-93 gasoline. When the engine load was decreased to pursue HCCI-like combustion in ultra-lean mixtures, NVO is the essential method especially for the low intake temperature and high anti-knock gasoline. However, to further approach the real application of SICI combustion, high CR and low octane number fuel as well as supercharger were emphasized by Urushihara et al. [38]. As mentioned above, most studies used relatively higher RON gasoline for SICI investigation without ethanol addition. Even though Sjöberg et al. [24, 25], Gentz et al. [30] and Hu et al. [31] have studied the performance of adding 30%, 10% and 85% (volume fraction) ethanol into gasoline, respectively, the RONs were more than 90 and quite high intake temperatures were required. Regarding the control of SICI combustion, Mendrea et al. [39] considered CA50 (crank angle of 50% mass fraction burned) to be the best indicator. Recently, Hunicz et al. [29] introduced a new parameter, which was calculated by 2CA50-CA95, to better describe the stability of SICI combustion with commercial gasoline with RON 95. However, the combustion characteristics of the cycles with high thermal efficiencies and its dependence on fuel type are still not clear. Using a single blending ratio could not comprehensively reveal the influence of ethanol on SICI combustion.

In regard to the effects of ethanol on particle number (PN) emissions, it has been well recognized that ethanol can reduce PN concentration and particle size in both SI and HCCI engines, which is due to the significant reduction of accumulation particles in well-mixed mixtures [40-46]. Even though the soot produced from ethanol-gasoline blends have a lower activation energy of oxidation compared with that from pure gasoline [15, 47] it should be emphasized that ethanol has a higher latent heat of vaporization and lower boiling point than most of the heavy components in gasoline, both of which would increase the risk of nucleation particle deterioration under low load

and heavy wall impingement conditions [15, 16, 43, 48]. Furthermore, compared to the SI mode, both Kaiser et al. [49] and Maurya et al. [50] found HCCI produced more accumulation mode particles under the same engine load. Meanwhile, Maurya also observed that ethanol had no obvious advantage in reducing accumulation mode particles [45] in HCCI combustion. Currently, only a few works have focused on the characteristics of PN emissions in SICI combustion especially for ethanol-gasoline blends. However, as a promising combustion mode that can achieve high efficiency, SICI deserves deep investigation on the effect of ethanol addition on PN characteristics, which is of practical significance to developing high efficiency engine.

The aim of this study is to systematically investigate the influence of ethanol on SICI engine performance including combustion characteristic, fuel economy and PN emissions. Ethanol-gasoline blends were formulated by two methods, which will be referred to as splash blending and RON-controlled blending respectively in the following sections. Ethanol-gasoline fuels prepared by splash blending have different ethanol contents, so the RON of the mixed fuel rises with increasing ethanol content, which can directly reflect the influence of ethanol. RON-controlled blending compares a blended fuel to another pure gasoline with the same RON, so it can reveal fuel-to-fuel interaction on auto-ignition [36, 37, 51]. Three base gasolines with different aromatics and olefins concentrations were prepared, indicating different unsaturation degrees. Two engine operating points were selected under different air dilution ratios and EGR conditions. Two dimensionless parameters were extracted from a mass of engine cycles working with various test fuels to describe the characteristics required for high thermal efficiency combustion. Not only PN emissions but also gaseous pollutants were measured to better analyze the special phenomenon of PN emissions in SICI combustion. Based on the experimental results, *T-p* trajectories coupled with ignition delay contours

were depicted to further seek the direction of optimization for combustion system. Ethanol's characteristics shown in the experiments could provide a fuel-design reference for the development of dedicated SICI engine.

Nomenclature

AHRA	auto-ignition heat release amount	LHV	lower heating value
ATDC	after top dead center	LTHR	Low temperature heat release
BMEP	brake mean effective pressure	MAPO	maximum amplitude of pressure oscillation
BSFC	brake specific fuel consumption	MBT	minimum spark advance for best torque
$BSFC_{eq}$	equivalent BSFC	MFB	mass fraction burned
BSNOx	brake specific NOx	MON	motor octane number
BSTHC	brake specific THC	NOx	nitrogen oxidizes
BTDC	before top dead center	NVO	negative valve overlap
CAi	crank angle of *i*% MFB	PAHs	polycyclic aromatic hydrocarbons
CI	compression ignition	PN	particle number
COV_{IMEP}	coefficient of variation of IMEP	PVO	positive valve overlap
CR	compression ratio	RCM	rapid compression machine
DOC	duration of combustion	RON	research octane number
EGR	exhaust gas recirculation	S	octane sensitivity
EOI2	end of second injection timing	SD	spark delay
FBHR	flame-based heat release ratio	SI	spark ignition
GHG	green-house gas	SICI	spark-ignition to compression-ignition
HCCI	homogenous charge compression ignition	SOI1	start of first injection timing
HRR	heat release rate	ST	spark timing
IMEP	indicated mean effective pressure	TGDI	turbocharged gasoline direct injection engine
ISFC	indicated specific fuel consumption	THC	total hydrocarbons
KI	knock intensity	TDC	top dead center

2. Methods

2.1 Experimental setup

The engine specifications are listed in Table 1 and the experimental setup is shown in Fig. 1. A 4-cylinder turbocharged direct injection (TGDI) engine with the CR of 12 was used in this work. The in-cylinder pressure was measured by a measuring spark plug integrated with a pressure sensor (Kister 6115C), then the pressure signal was sampled and processed by a combustion analyzer (Kistler Kibox). With the real-time analysis on pressure and crank angle signal, the heat release rate (HRR), combustion phasing including CA2, CA10, CA50 and CA90 (CA*i*, the crank angle of *i*% mass fraction burned), and coefficient of variation could be obtained. An ETAS INCA 7.2 engine control system was used to provide flexible adjustment in spark timing (ST), injection timing, EGR rate and excess air ratio (λ). The high-pressure EGR was adjusted by one proportional valve, and the temperature of EGR was kept at about 50 °C. The fuel amount consumed per engine cycle was determined by λ and the opening of throttle. The fuel consumption rate was measured by a volume flow meter. The temperatures and pressures of all fluids were recorded by the data acquisition system, and both the coolant and lubricating oil were maintained at 85 °C. A DMS500 was used to measure PN and particle spectrum characteristics. During the PN measurement, the first-stage dilution ratio was fixed to 5.0 while the second-stage dilution ratio was adjusted to balance the signal to noise ratio and adapt varied engine operating conditions. The conventional gaseous emissions including THC and NOx were measured to assist PN analysis. During the engine test, pressure trace of 200 consecutive cycles was recorded along with one-minute data acquisition for emissions and fuel consumption in each operating condition. To extend the lean limit for SICI combustion, the heater for fresh intake air was used. The uncertainty of the main test variables can be found in Table 2.

Table 1
Engine specifications

Parameter	Value
Bore (mm)	73
Stroke (mm)	88.2
Connecting rod (mm)	141.4
Compression ratio	12
Injection pressure (MPa)	35
Fuel injection mode	Direct injection

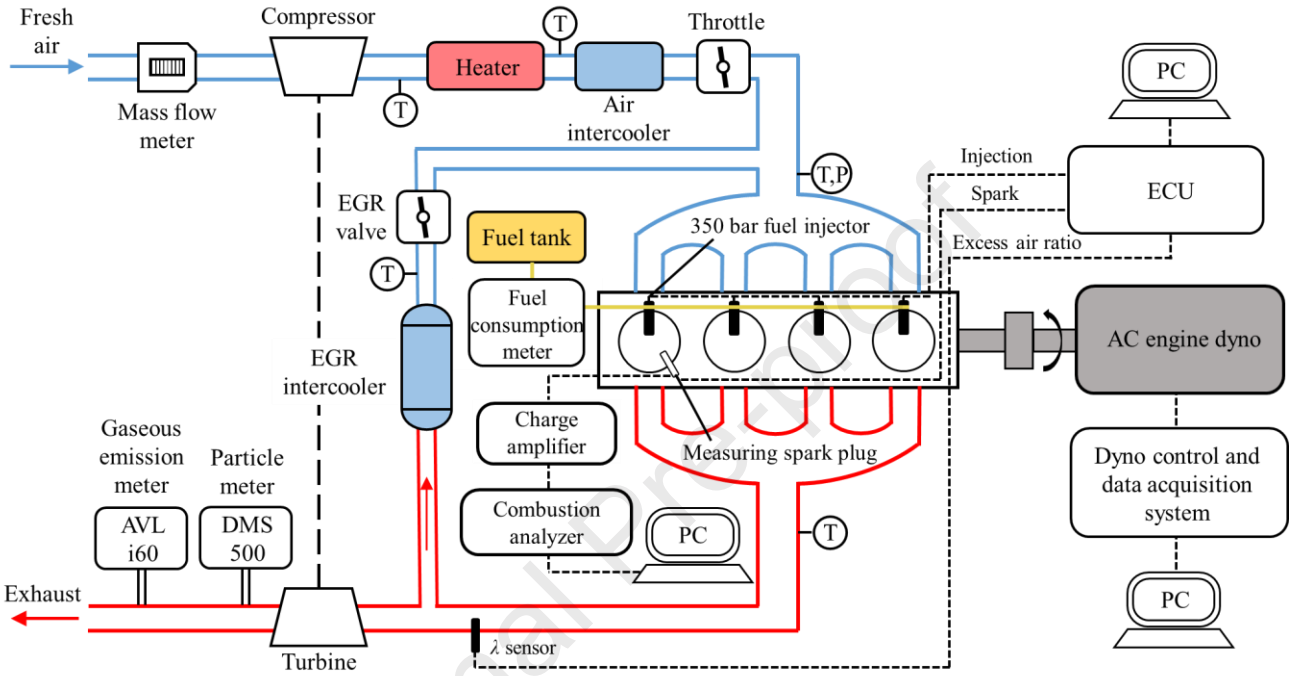

Fig. 1 The schematic of engine test bench

Table 2

The measured parameter and experimental uncertainty

The measured parameter	Test device	Uncertainty (%)
In-cylinder pressure (MPa)	Kistler 6115C	±0.01
Dyno torque (N·m)	HBM torque flange	±0.2
Engine speed (r/min)	Crank-shaft encoder	±0.5
Fuel volume flow (cm^3/min)	MAX P213	±0.2
Air flow meter (kg/h)	ToCeil 20N	±0.2
Intake and exhaust temperature (K)	K-type thermocouples	±1
Gaseous emissions (ppm)	AVL i60	±1
Excess air ratio	NTK oxygen sensor	±0.1
Particle number (#/cm^3)	Cambustion DMS500	±1

2.2 Fuel properties and operating conditions

The properties of three base gasolines (70#, 82# and 93#) along with ethanol were listed in Table 3. The main difference in octane number of these three base gasolines is caused by around 10%

aromatic content increment between each other. Considering high RON of ethanol, 5%, 10% and 15% volume fractions of ethanol were selected to blend with the 70#. This kind of blending will be referred to splash blending [52]. Another blending method needs to control the octane number of mixed fuels based on the blending model [10, 14]. In this study, 82# and 70#E10 have the nearly identical RON and S, which can reflect ethanol impact in fuel type separately on SICI combustion by ruling out octane number influence and can simultaneously verify the synergistic effects on auto-ignition observed in RCM [51] through the engine test.

Table 3

Property of basic components of test fuel in engine experiments

Property	70#	82#	93#	Ethanol*
RON	70.1	81.0	93.4	108.5
MON	69.4	77.0	83.3	90.7
S (RON-MON)	0.7	4.0	10.1	17.8
LHV (MJ/kg)	43.26	43.30	42.64	26.95
Density@293 K (g/cm^3)	0.7251	0.7302	0.7471	0.79
Aromatics (%, v/v)	10.46	19.32	29.26	0
Olefins (%, v/v)	9.41	12.80	11.62	0
T_{10} (°C)	59.2	54.4	60.6	78
T_{50} (°C)	102.4	101.8	106.3	
T_{90} (°C)	135.9	148.8	162.4	
T_{end} (°C)	164.3	186.1	197.8	
C (%, m/m)	85.27	85.90	86.67	52.17
H (%, m/m)	14.73	14.10	12.50	13.04
O (%, m/m)	0	0	0.83	34.78

* Ethanol properties are consistent with Foong et al. [53]

Engine test conditions for each fuel were listed in Table 4. Two operating points, 0.5 MPa BMEP @1500 r/min and 0.8 MPa BMEP @2000 r/min were chosen for the SICI experiments, which are the common working conditions for engines on hybrid vehicles. Among them, 70#, 70#E5, 70#E10 and 70#E15 were used under air dilution conditions at 1500 r/min and meanwhile, 70#, 70#E10 and 82# were used under EGR condition at 1500 r/min and 2000 r/min. The selection of λ (1.0-1.6) and EGR (0-25%) in experiments should avoid misfire. Since SICI combustion comprises

of two stages: flame propagation and end-gas autoignition, it is meaningful to study the effect of ethanol on combustion and PN emissions during the stage of flame propagation, which was carried out under pure SI mode with 93# and 93#E10. Double injection and intake temperature of 50 °C were conducted unless specified. The start of the first injection (SOI1) and the end of the second injection (EOI2) was fixed at -300 °CA and -160 °CA ATDC, respectively. The split ratio was kept at 3:2 to minimize the risk of PN deterioration and maintain the degree of fuel stratification simultaneously, conducive to flame acceleration [48, 54] in lean conditions. The aforementioned injection strategy has been validated by 3-D simulation and preliminary experiments.

Table 4
Engine control strategy for test fuels

Fuel type	70#	70#E5	70#E10	70#E15	82#	93# and 93#E10
T_{in} (℃)	50	50	50	50, 80	50	30
p_{in} (MPa)	0.1	0.1	0.1	0.1	0.1	0.1
λ	1.0, 1.2, 1.4	1.0, 1.2, 1.4	1.0, 1.2, 1.4	1.0, 1.2, 1.4, 1.6	1.0, 1.2, 1.4	1.0. 1.2, 1.4
SOI1 (°CA ATDC)	-300	-300	-300	-300	-300	-310--90 or -300
EOI2 (°CA ATDC)	-160	-160	-160	-160	-160	w/o or -280--60
Split ratio	3:2	3:2	3:2	3:2	3:2	3:2
EGR (%)	0-25%	/	0-25%	/	0-25%	0-25%
Speed (r/min)/ BMEP (MPa)	1500 / 0.5 2000 / 0.8	1500 / 0.5	1500 / 0.5 2000 / 0.8	1500 / 0.5	1500 / 0.5 2000 / 0.8	1500 / 0.5 2000 / 0.8

2.3 Parameter definition

2.3.1 Knock intensity

Knock characteristic in SICI combustion was evaluated by the integral-type knock intensity (KI) as shown in Eq. (1). In this study, if one engine cycle has the maximum amplitude of pressure oscillation (MAPO) more than 0.2 MPa, it would be regarded as a knocking cycle. The first-order oscillation frequency given by the “drum” mode [55] was 7.2 kHz for this engine, so the cut-off

frequency of the high-pass filter was set to 6 kHz. For one operating point, if the proportion of knocking cycles is over 10% to the recorded 200 consecutive cycles, this point would be considered as a knocking condition. The operating point with 10% knocking cycles was the critical condition and its KI was seen as knock threshold.

Fig. 2 shows an example to obtain the knock threshold. The MAPO and the integration between p_{filter} and crank angle for each cycle were first calculated in each operating point including 200 consecutive cycles, and then the average of MAPO and p_{filter}-φ integration (i.e. KI) of 200 cycles were taken, demonstrated in Fig. 2 (b). It is clear that the amount of knocking cycles increases with advanced spark timing and the critical condition occurs when ST is -38 °CA ATDC, as shown in Fig. 2 (a). The KI under the critical condition was defined as the knock threshold, which is about 0.5 °CA·MPa and independent of operating conditions. The corresponding average-MAPO under the critical condition is near 0.1 MPa, usually selected as the criterion of knock in SICI combustion as well [6]. Therefore, KI = 0.5 °CA·MPa regarded as the knock threshold was rational in this study.

$$KI = \frac{\sum_{i=1}^{n}\int_{\varphi_1}^{\varphi_2}\left|p_{\text{filter}}^{i}\right|\cdot \mathrm{d}\varphi}{n} \tag{1}$$

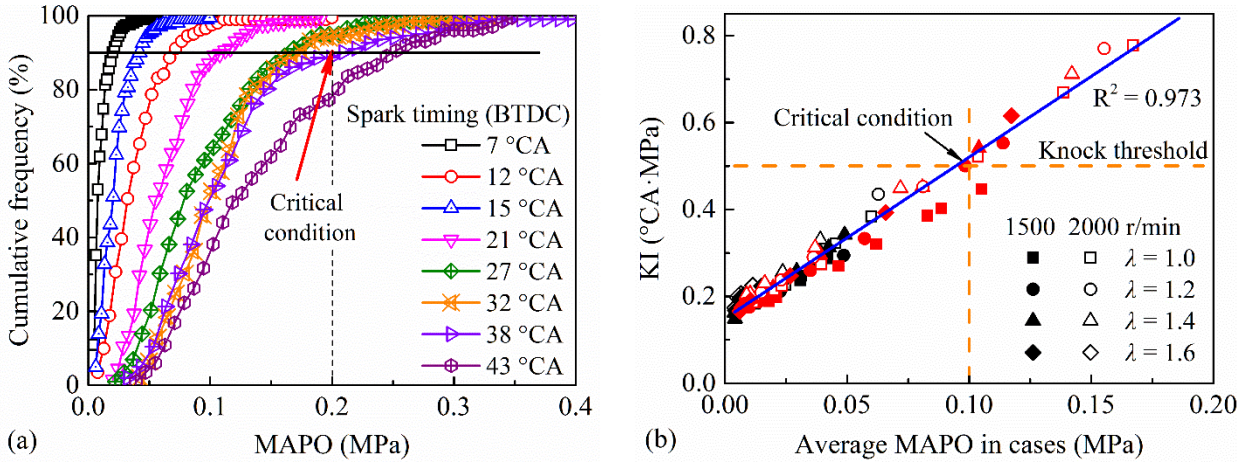

Fig. 2 The principle of selecting knock threshold

2.3.2 Fuel consumption and energy balance analysis

Because of the difference in LHV between base gasolines, the LHV of mixed fuel varies a lot with different blend ratio. The equivalent BSFC ($BSFC_{eq}$) relative to 82# was used in this study, which can be calculated using Eq.(2) where Y_{Eth} and Y_{Base} are the mass fractions of ethanol and base gasoline in the mixed fuel, respectively.

$$BFSC_{eq} = BFSC_{real} \cdot \frac{H_{u\_Eth} \cdot Y_{Eth} + H_{u\_Base} \cdot Y_{Base}}{H_{u\_82\#}} \tag{2}$$

Based on the first law of thermodynamics, the chemical energy contained in supplied fuels is generally divided into four parts during combustion: engine work (gross indicated work), combustion loss, exhaust loss and heat transfer loss, which can be calculated using Eq. (3)-(6) [56, 57].

$$\eta_{ig} = \frac{W_{i\_gross}}{m_f \cdot H_u} \tag{3}$$

$$\eta_c = 1 - \frac{\dot{m}_{CO} H_{u\_CO} + \dot{m}_{THC} H_u}{\dot{m}_f \cdot H_u} \tag{4}$$

$$\eta_{exhaust} = \frac{\dot{m}_{out}\left[h_{out}\left(T_{out}\right) - h_{in}\left(T_{in}\right)\right]}{\dot{m}_f \cdot H_u} \tag{5}$$

$$\eta_{heat\_transfer} = 1 - \eta_{ig} - \eta_{exhaust} - \left(1 - \eta_c\right) = \eta_c - \eta_{ig} - \eta_{exhaust} \tag{6}$$

where η_{ig}, η_c, $\eta_{exhaust}$ and $\eta_{heat\_transfer}$ are the gross indicated thermal efficiency, combustion efficiency, exhaust loss and heat transfer loss, respectively. H_u and H_{u_CO} are the LHVs of the test fuel and carbon monoxide. m_f is the fuel injection amount per cycle and $\dot{m}_f$ is the fuel injection rate ($\dot{m}_f = m_f \cdot n/120$).

2.3.3 Combustion characteristic timing and heat release ratio

Based on the HRR profile, auto-ignition timing (φ_{auto}) was identified as the maximum curvature position of HRR [4], which is more sensitive to the first peak of d^2p/dt^2 [36]. As seen in Eqs. (8)-(9), the heat release amount from the start of combustion to φ_{auto} divided by the total energy supplied in

one cycle is defined as the flame-based heat release ratio (FBHR). The rest of the energy amount is released during the auto-ignition stage, called auto-ignition heat release amount (AHRA). Spark delay (SD) is defined as the interval between the spark timing and CA10 while the duration of combustion (DOC) is calculated by CA90-CA10. The aforementioned characteristic parameters are depicted in Fig. 3.

$$\frac{\mathrm{d}Q}{\mathrm{d}\varphi}=\frac{\gamma}{\gamma-1}p\frac{\mathrm{d}V}{\mathrm{d}\varphi}+\frac{1}{\gamma-1}V\frac{\mathrm{d}p}{\mathrm{d}\varphi} \tag{7}$$

$$FBHR=\int_{\varphi_{\min}}^{\varphi_{\mathrm{auto}}}\frac{\mathrm{d}Q}{\left(m_{\mathrm{f}}\cdot H_{\mathrm{u}}\right)\mathrm{d}\varphi} \tag{8}$$

$$AHRA=1-FBHR \tag{9}$$

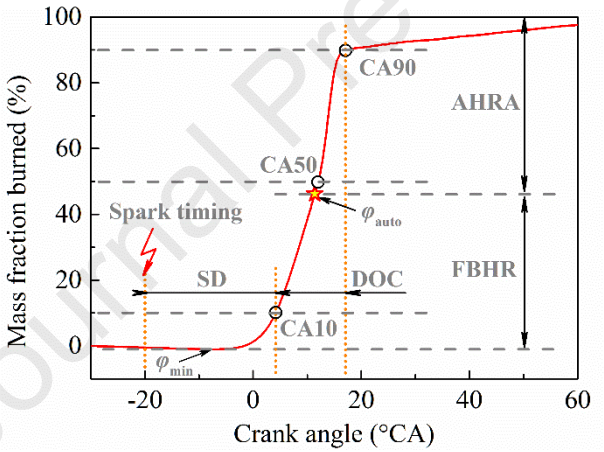

Fig. 3 Definition of combustion characteristic parameters

3. Results and discussion

The characteristics of combustion, fuel economy and pollutant emission were analyzed using the two ethanol blending methods under air dilution and EGR conditions. Based on the ethanol performance in SICI combustion, *T-p* trajectories coupled with contours of the overall ignition delay were plotted to further reveal the mechanism of aforementioned experimental result and help seek the direction of engine improvement.

3.1 Combustion characteristics

3.1.1 In-cylinder pressure and heat release rate

Fig. 4 shows the profiles of in-cylinder pressure and HRR at MBT (Minimum spark advance for best torque) under air dilution and EGR conditions. Fig. 4 (a), (c) and (e) reflect the effects of ethanol with splash blending at 1500 r/min and 0.5 MPa BMEP while Fig. 4 (b), (d) and (f) represent the effects of ethanol with RON-controlled blending at 2000 r/min and 0.8 MPa BMEP. The φ_{auto} is marked by a "circle" in each curve. It is clear that as the ethanol content increases from 0 to 15%, combustion phasing is advanced for each λ. This is attributed to two factors. Firstly, the knock tendency is restricted by ethanol's high RON and S [14] so that the spark timing can be advanced. On the other hand, ethanol has faster laminar flame speed and stronger pressure dependence of flame speed than aromatics and alkanes [51, 58]. As the ethanol content gets higher, the maximum HRR decreases and φ_{auto} approaches closer to the top dead center. However, the advanced degree of φ_{auto} gets lower in the leaner mixture because the effect of advanced spark is weakened when the ignition delay time of the end-gas gets longer.

For the EGR condition (λ = 1.0), the aforementioned results can also be found in the comparison between 70# and 70#E10. Moreover, by comparing 70#E10 with 82#, the advantage of flame speed of 70#E10 gradually loses as the EGR rate rises. The auto-ignition intensity decreases significantly and φ_{auto} also gets delayed drastically. Both phenomena can be attributed to ethanol's high sensitivity to exhaust dilution [36]. That is to say, ethanol has low EGR tolerance, and the flame propagation along with the reactivity in ethanol-gasoline mixtures becomes more significantly restricted with increasing EGR rate. Therefore, fuels with ethanol blending are not suitable for highly exhaust-diluted SICI combustion.

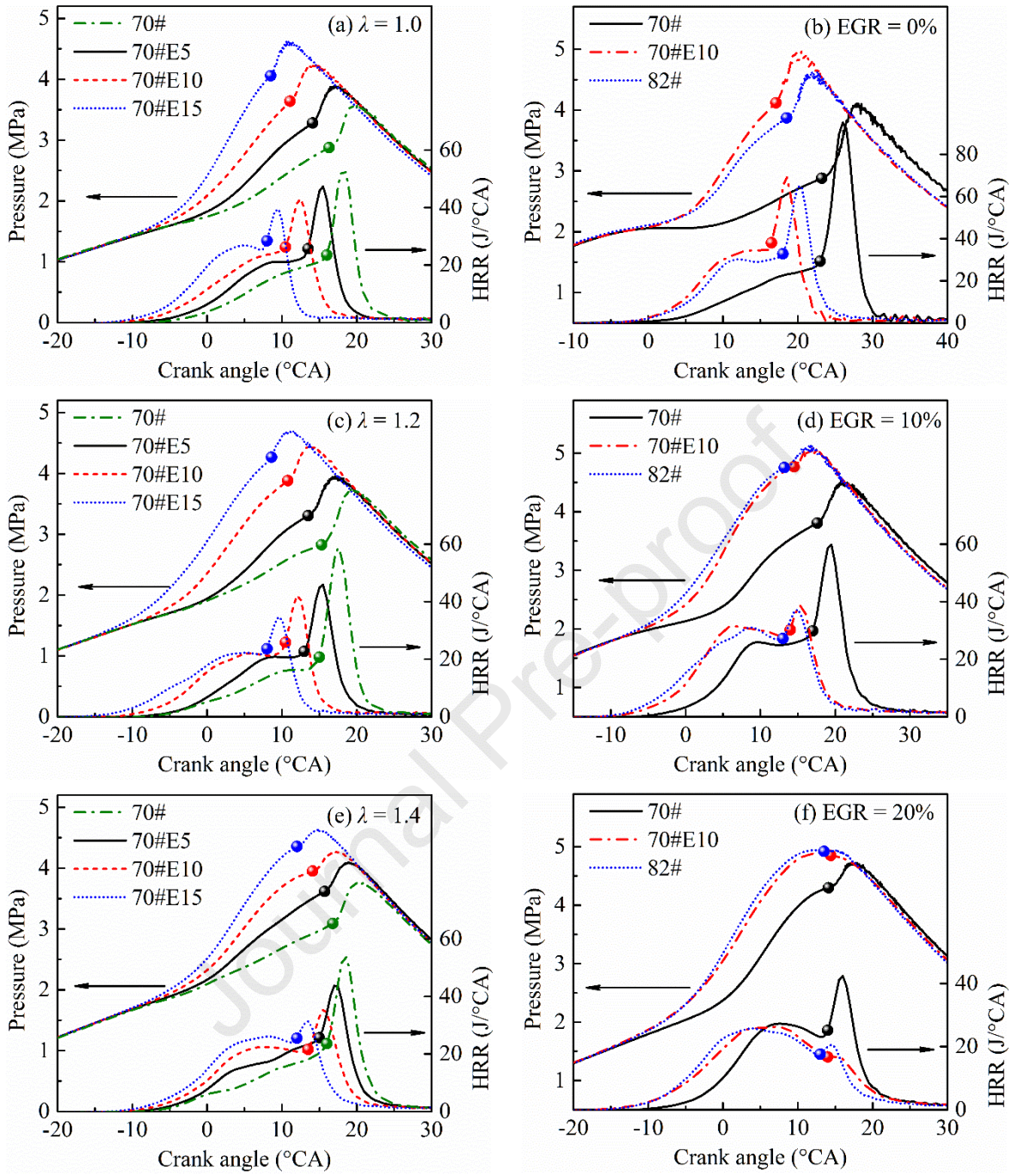

Fig. 4 Pressure and HRR profiles in air dilution and EGR conditions using two blending methods

Fig. 5 compares the combustion phasing of various operating conditions shown in Fig. 4. The "circles" represent CA50 for each fuel. The "stars" in Fig. 5 (a) represent the fuel with the best fuel economy, i.e. 70#E15, while the "stars" in Fig. 5 (b) and (c) represent the EGR rate with the best fuel economy. It can be well recognized that for the low engine load (1500 r/min and 0.5 MPa BMEP), the "stars" belongs to the cases with the most advanced CA50, which means that fuel consumption is

closely related to CA50 rather than auto-ignition timing. However, with the increase of engine speed and BMEP, the CA50 earlier than 10 °CA ATDC could not provide a better fuel economy, indicating that fuel consumption is strongly dependent on the relative position of CA50 in the entire combustion cycle. A quantitative discussion on the requirements of combustion parameters under high thermal efficiency conditions will be presented in the following section. It can also be seen that the SDs of the fuels with high ethanol content is larger than those of non-oxygenated fuels under highly diluted conditions (EGR = 25% and λ = 1.4), which further supports the fact that ethanol has lower dilution tolerance, and more advanced spark timing are required to maintain CA50 not deviated much.

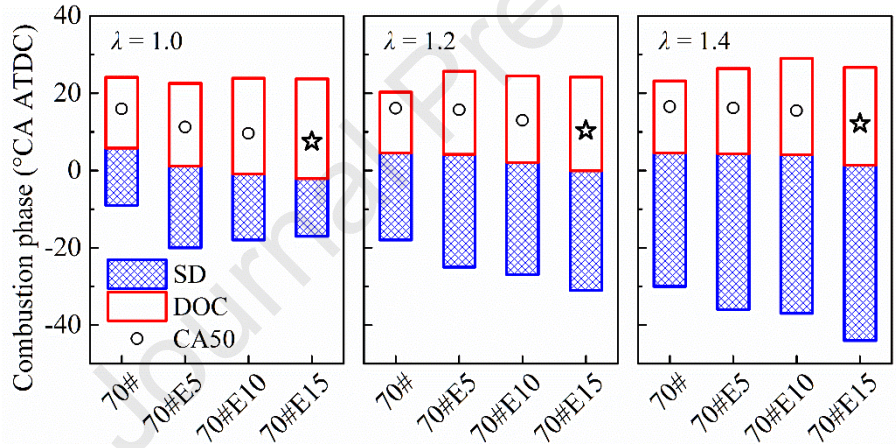

(a) 1500 r/min 0.5 MPa BMEP air dilution conditions

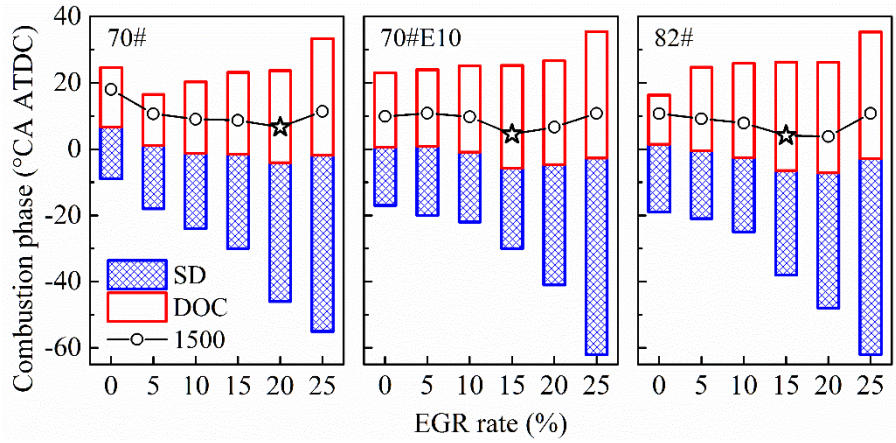

(b) 1500 r/min 0.5 MPa BMEP EGR conditions

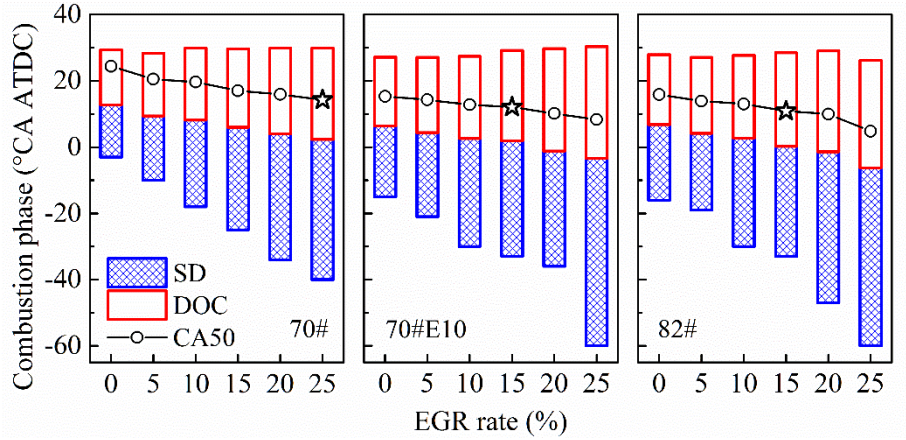

(c) 2000 r/min 0.8 MPa BMEP EGR conditions

Fig. 5 Comparison of combustion phases in SICI combustion with different test fuels

Fig. 6 further displays the distribution of combustion phasing under air dilution and EGR conditions at the same engine load as Fig. 4 when sweeping the spark timing until the KI is over the threshold or CA50 is ahead of TDC. Shorter CA50-CA10 and CA90-CA50 can be regarded as the indicators of faster flame propagation and stronger auto-ignition intensity, respectively. It is clear that for air dilution, when CA50-CA10 gets shorter as the spark timing advances, the duration of CA90-CA50 declines firstly and then increase, which is more obvious when λ is near stoichiometric. This indicates that too early spark timing has a negative influence on the combustion phasing control especially for the fuels with high ethanol content. Due to the low chemical reactivity of ethanol, to obtain the best fuel economy, an advanced spark timing should be used when switching the fuel from 70# to 70#E15 (shown in Fig. 5), but the allowable spark timing range is narrow. Low EGR tolerance of ethanol can be well recognized from Fig. 6 (b), (d) and (f). Both CA50-CA10 and CA90-CA50 of 70#E10 gradually increase with EGR with larger steps than 70# and 82#, indicating the exhaust dilution has a more significant impact on flame propagation and auto-ignition of 70#E10 compared with the other two fuels.

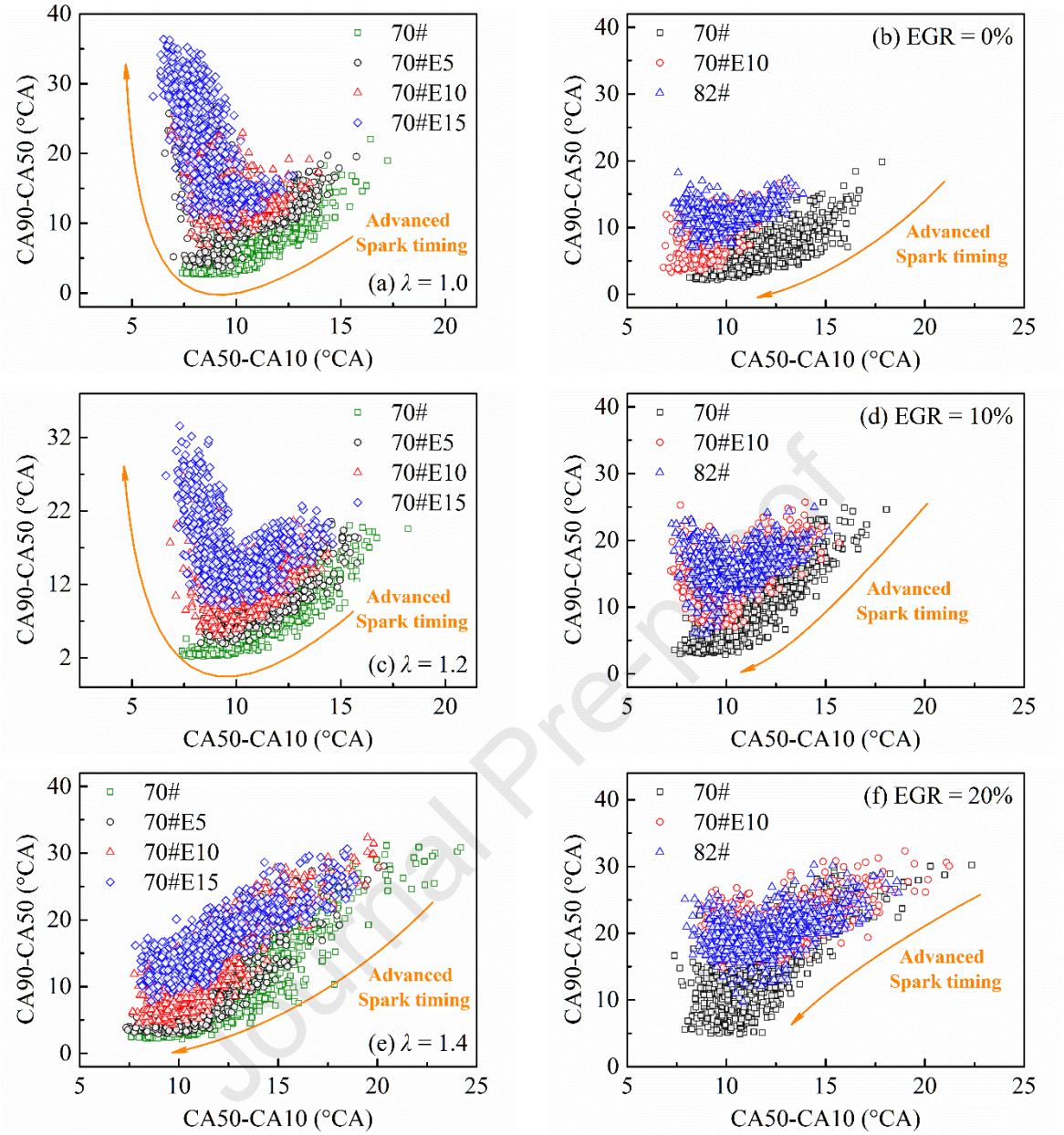

Fig. 6 Distribution of combustion phasing against spark timing sweep under air dilution and EGR conditions

3.1.2 Ethanol impact on knock characteristic in SICI

Fig. 7 and Fig. 8 depict the effect of ethanol on KI under air dilution and EGR conditions, respectively. Under air dilution conditions, ethanol addition shows anti-knock performance for the splash blending fuels as depicted in Fig. 7 (a)-(c), while the synergistic effect on auto-ignition is also pronounced in the RON-controlled fuels as seen in Fig. 7 (d). Based on the current engine specifications and intake thermodynamic states, the temperature at TDC is not more than 800 K. This means that ethanol plays the key role in knock resistance in splash blending, so KI decreases as the

ethanol content increases from 0 to 15%, corresponding to a RON value rise from 70 to 85. A similar observation could also be found in Ref. [25] in which the peak-to-peak pressure oscillation of E30 is only about 40% of alkylates at the same CA50. This result indicates ethanol has a strong ability to reduce low temperature heat release (LTHR) produced by low-S components through fast consumption of OH radical [14, 59]. As for Fig. 7 (d), because the two fuels have the same RON, the synergistic effect on auto-ignition is attributed to more HO_2 production from ethanol followed by faster consumption by benzyl [51, 60]. This synergistic effect can also be supported by the shorter CA90-CA50 of 70#E10 compared to 82# under the higher engine load as shown in Fig. 6 (b). It should be noted that if the amount of added ethanol is too much, e.g., twice more than aromatic's content, the LTHR restriction from ethanol will be dominant [25].

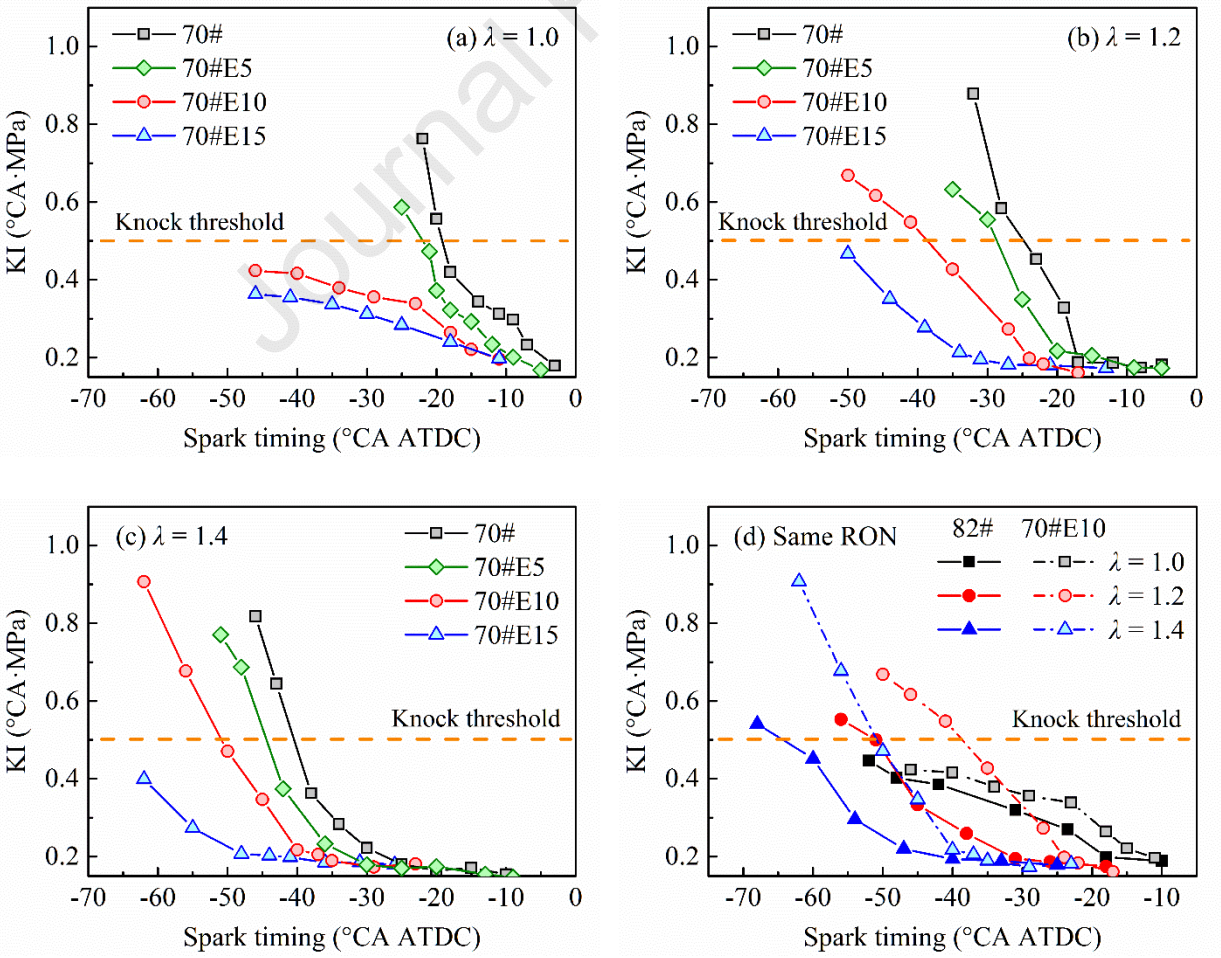

Fig. 7 Effect of ethanol blending on knock intensity under air dilution conditions

The similar phenomenon of ethanol's anti-knock performances and synergistic effects can also be seen under EGR conditions shown in Fig. 8. The KI of 70# is significantly larger than those of 70#E10 and 82# except for the cases with the highest EGR rate under low engine loads. The KI of 70#E10 is always slightly larger than that of 82# until the EGR rate gets more than 20% where their KIs are almost identical due to the low EGR tolerance of ethanol [36]. CA50 has a positive correlation with KI for all fuels. To describe the EGR tolerance more quantitatively, the dependence of KI on CA50 is defined by Eq. (10), and the corresponding result can be seen in Fig. 9 below.

$$\beta = \left| \frac{\partial KI}{\partial \mathrm{CA50}} \right|_{\max} \tag{10}$$

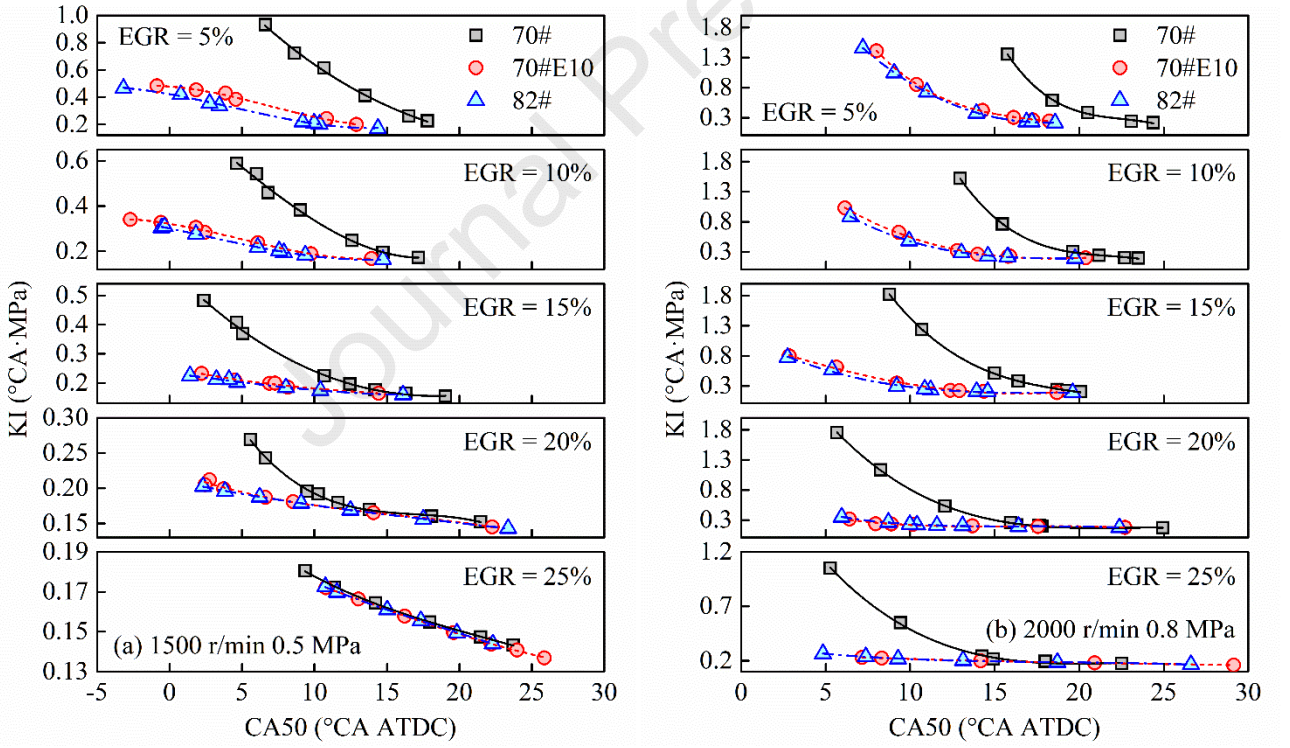

Fig. 8 Effect of ethanol blending on knock intensity in EGR conditions

It can be seen from Fig. 9 that 70# has the largest dilution tolerance and ethanol addition by splash blending can significantly decrease β. The lower β value, the weaker trade-off between KI and CA50, which is conducive to fuel economy improvement. Specifically, for the comparison between

70# and 70#E10, when the EGR rate increases from 5% to 15% the difference in β between 70# and 70#E10 is 64.8%, 71.1%, 78.4% (1500 r/min) and 31.2%, 56.6%, 87.6% (2000 r/min), respectively. Moreover, comparing 70#E10 with 82#, the β value of 70#E10 is larger than that of 82# when the EGR rate is less than 15%, but it becomes lower when EGR is over 15%, which is also a reflection of the low dilution tolerance of ethanol. In that case, the weak flame propagation is hard to effectively adjust combustion phasing and further influence KI. Consequently, a larger drop of β value occurs for 70#E10 (92.2% at 1500 r/min and 98.2% at 2000 r/min) compared to 82# (87.7% at 1500 r/min and 94.1% at 2000 r/min) when the EGR rate rises from 5% to 25%.

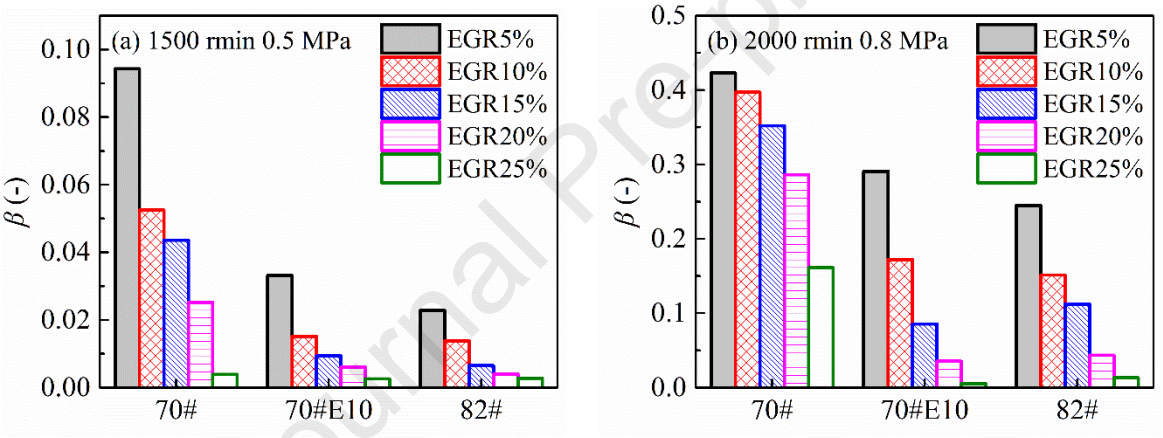

Fig. 9 Dependence of KI on CA50 under EGR conditions

3.2 Fuel economy using fuels with varied RON and ethanol content

Fig. 10 compares $BSFC_{eq}$ of the test fuels under air dilution conditions considering the influence of ethanol amount, combustion mode and intake temperature. Double injection was used in all SICI cases shown in Fig. 10. The $BSFC_{eq}$ of 93# under SI mode with single and double injection strategies were selected as the reference. For the effect of ethanol on fuel economy, it is clear that the increase of ethanol allows CA50 to move towards TDC, and the CA50 with the best fuel economy condition locates in the range of 10-15 °CA ATDC regardless of ethanol contents.

For the effect of combustion mode on fuel economy, SICI can optimize CA50 in contrast to SI

regardless of injection strategy, improving fuel economy except the cases with 70# due to its too high reactivity which is impossible to adjust CA50 to approach TDC too closely. Specifically, comparing SICI with single-injection SI, double injection used in SICI can form fuel stratification and shorten DOC because of auto-ignition portion, which is beneficial to flame acceleration and heat loss reduction. Therefore, the minimum $BSFC_{eq}$ of SICI is much lower than single-injection SI compared to double-injection SI. However, this advantage of double injection over single injection in SI mode gets weak with the lean mixture and disappears at λ = 1.4 because of the extended DOC and the deteriorated flame stability of an over-lean mixture. In this situation, compression ignition shows the potential to reduce fuel consumption. The maximum improvement in $BSFC_{eq}$ between SI and SICI is less than 5 g/kW·h at λ = 1.0 but significantly increases to 15-25 g/kW·h at λ = 1.4. Fig. 10 (d) further compares the $BSFC_{eq}$ of 70#E15 with various λs at T_{in} = 50 °C and 80 °C. It can be recognized that increasing T_{in} could not lower the minimum $BSFC_{eq}$ as long as the CA50 is in the range of 10-15 °CA ATDC. Fig. 10 (d) also shows that leaner mixture results in lower $BSFC_{eq}$ which can be as low as 220 g/KW·h at λ = 1.6.

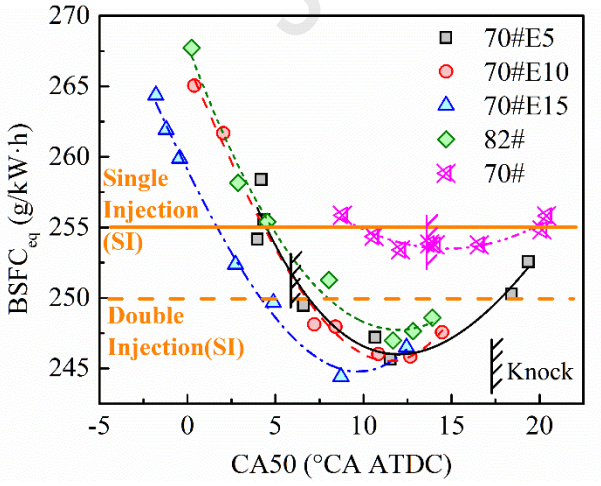

(a) λ = 1.0

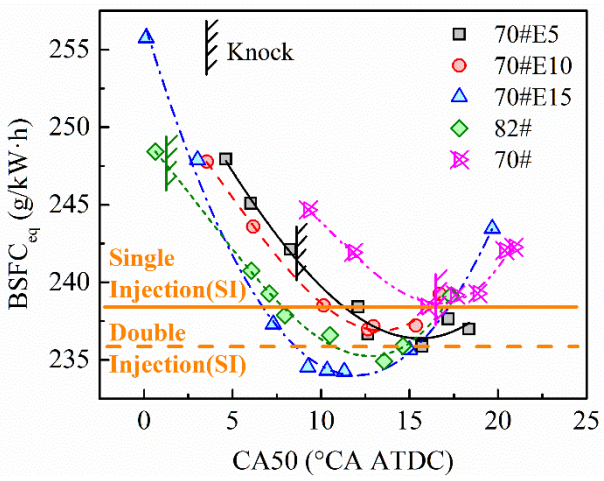

(b) λ = 1.2

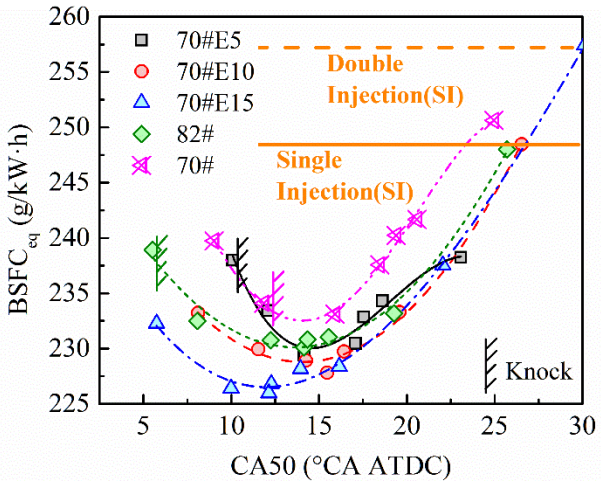

(c) λ = 1.4

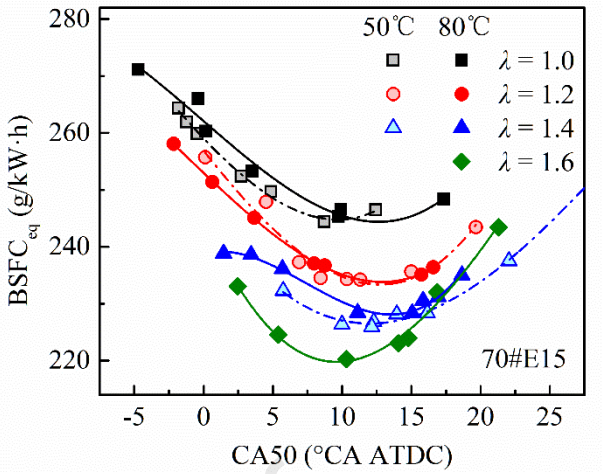

(d) BSFC$_{eq}$ at two T_{in}

Fig. 10 Fuel consumption of SICI under air dilution (1500 r/min, 0.5 MPa BMEP)

SICI combustion with the advantage in BSFC$_{eq}$ compared to SI under heavily diluted conditions can be found in Fig. 11. The strong knock tendency of 70# at the high load further restricts CA50 compared to the cases at the low load, and the fuel economy of 70# is even worse than SI which uses the same double injection strategy. At the EGR rate= 5% and 10%, the minimum BSFC$_{eq}$ of 70#E10 is lower than 82#, which is attributed to the more advanced combustion phasing and shorter DOC as shown in Fig. 6 (b). However, with the EGR rate over 10%, the low dilution tolerance of ethanol results in a higher BSFC$_{eq}$ of 70#E10 in contrast to 82#. Low dilution tolerance of ethanol decreases the control authority of combustion phasing [24] , and in this situation, the effect of advanced spark timing on fuel consumption reduction is also significantly weakened. In summary, based on Fig. 10 and Fig. 11, SICI combustion can extend dilution limit and improve fuel economy, meanwhile, low ethanol addition into hydrocarbon fuels can further decrease fuel consumption in SICI combustion.

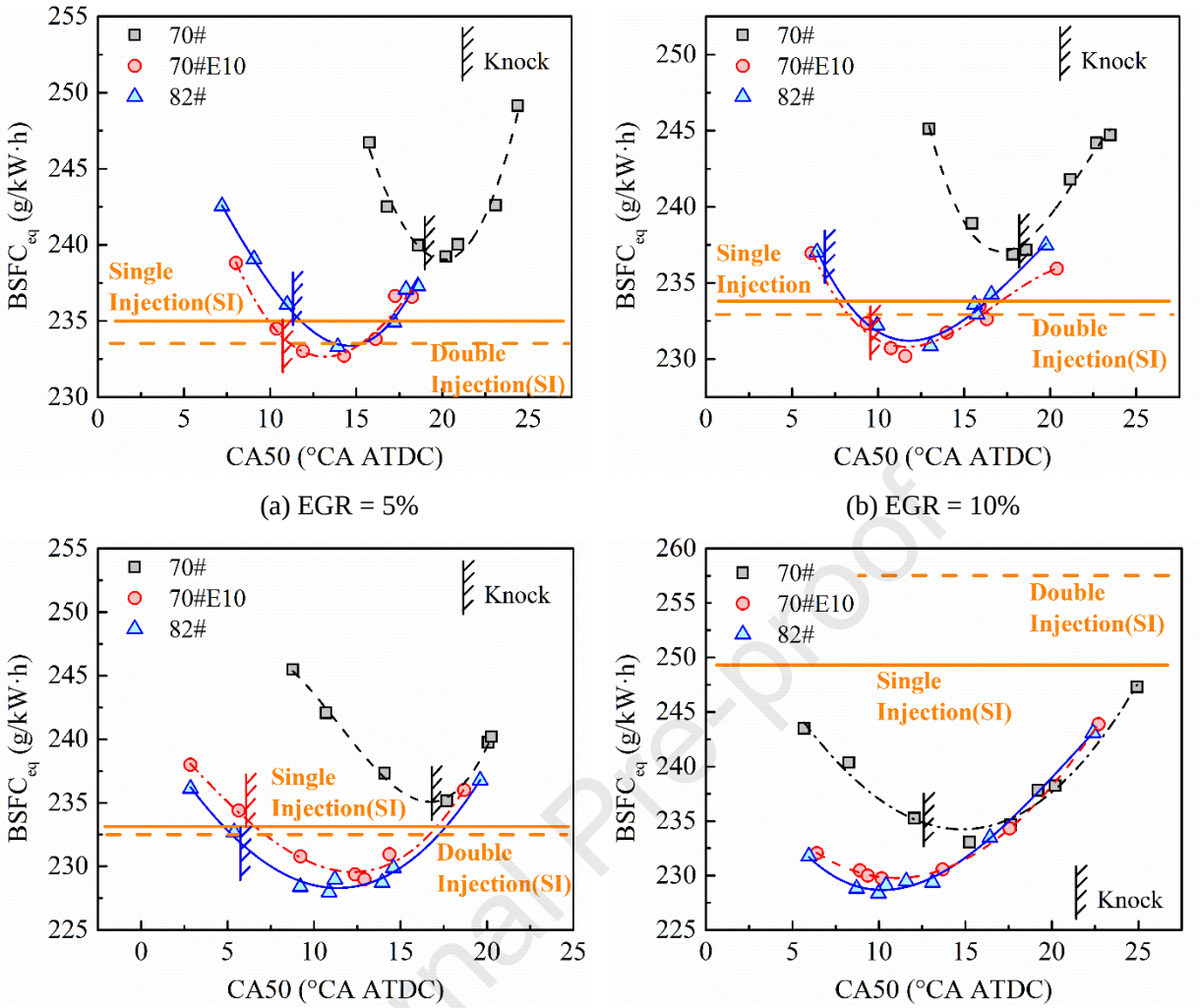

Fig. 11 Fuel consumption of SICI under EGR conditions (2000 r/min, 0.8 MPa BMEP)

Fig. 12 shows the results of energy balance analysis for λ = 1.4 with EGR = 5% and 20%. It can be seen that under air dilution and EGR conditions, the ratio of heat transfer loss is more than 30% because the heat transfer duration is lengthened under dilution combustion. The proportion of heat transfer will be further increased under low EGR condition due to the higher combustion temperature and enhanced heat transfer through the boundary layer in the occurrence of pressure wave oscillation [17], which is more prominent for 70# with stronger knock tendency. Lower heat transfer loss of ethanol-gasoline blend than alkylates under SICI mode could also be observed in Ref. [25] though higher-RON fuels were used. As for the exhaust loss, it is larger under EGR conditions (λ = 1.0) than under lean-burn because of the heavier thermal load. The larger exhaust and incomplete combustion

loss of 93# than any other fuels at λ = 1.4 is ascribed to the serious late burning and retarded combustion phasing.

Comparing lean-burn with EGR for 70#E10, even though the heat transfer loss is higher under lean-burn, the lower exhaust temperature along with the rich-oxygenated environment results in much less combustion loss and exhaust loss. Therefore, η_{ig} under lean burn is larger than that under EGR conditions. Considering the lower engine speed and load in lean burn, the proportion of fiction and pumping loss increases, so brake thermal efficiencies under λ = 1.4 and two EGR conditions are similar.

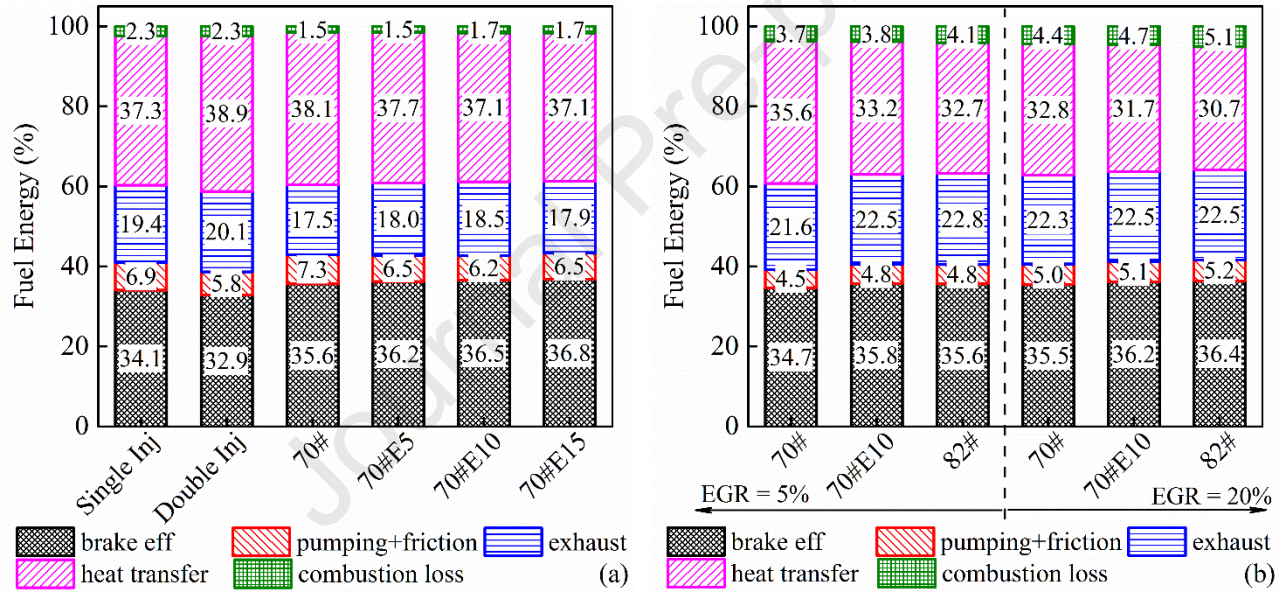

Fig. 12 Energy balance for different fuels under air dilution and EGR conditions

As depicted in Fig. 5, the relative position of CA50 in the entire combustion duration has a strong influence on fuel consumption under SICI mode. To further reveal the influence of the relative position of CA50, two dimensionless parameters, AHRA divided by FBHR and (CA90-CA50) divided by (CA50-CA10) were proposed. The former means the ratio of heat release amount from flame propagation to that from auto-ignition, and the latter can approximately represent the time ratio of flame propagation to auto-ignition. Fig. 13 (a) and (b) show the correlation between the two

parameters under air dilution and EGR conditions, respectively, in which the colorful data points are extracted from the cycles with more than 90% of the maximum η_{ig} for each fuel, and the gray points represent the cycles with lower efficiencies. For those high-efficiency cycles, it is obvious that the AHRA/FBHR can be well correlated with the (CA90-CA50)/(CA50-CA10) through exponential fitting. Moreover, using the exponential form for auto-ignition timing control can well adapt the variation of engine operation or fuel type even though its computational cost is higher than linear-fit model [61]. In the comparison between Fig. 13 (a) and (b), it shows that AHRA/FBHR changes more rapidly with (CA90-CA50)/(CA50-CA10) under EGR than under air dilution when the (CA90-CA50)/(CA50-CA10) is beyond 1.0, which means EGR can more significantly inhibit auto-ignition tendency and reduce heat release during the compression ignition stage compared to air dilution. In other words, spark timing has strong control authority on combustion phasing and can effectively maintain AHRA under air dilution conditions. However, this control authority gets significantly weak when using EGR. A rapid decline in AHRA still occurs even with much advanced spark timing as the EGR rate increases.

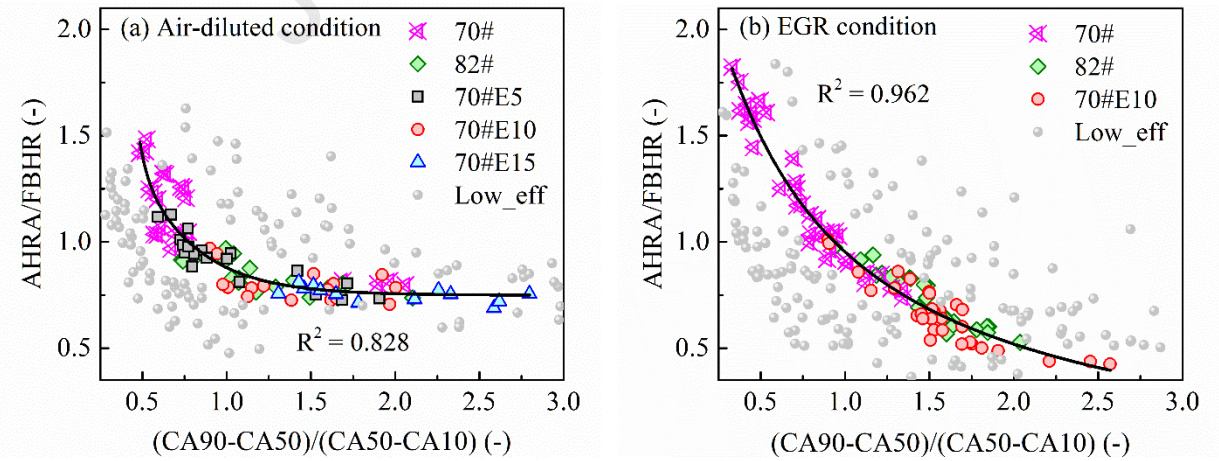

Fig. 13 The characteristics of engine cycles with high thermal efficiency under SICI mode at 1500 r/min

3.3 Particle number emissions

3.3.1 Effect of ethanol on PN in SI

In order to separate the influence of deflagration (flame propagation) portion and auto-ignition portion on PN emission in the entire SICI combustion event, this section firstly focuses on the effect of blending ethanol on PN emission under pure deflagration mode (SI). It is shown in Fig. 14 that compared with 93#, 93#E10 can decrease PN in both accumulation (D_p > 30 nm) and nucleation mode (D_p < 30 nm) when sweeping EOI2 for the double injection strategy. For the single injection, except for the severe wall impingement conditions (SOI1 = -310 and -90°CA ATDC), 93#E10 also has the ability to reduce accumulation mode particles. Whatever the number of injection is, both THC and PN deteriorate when the injection timing is too late, which indicates that the injection timing plays a more important role in emissions compared with the number of injection [18]. Moreover, under the relatively well-mixed conditions regardless of injection strategy, the decrease degree of accumulation particles is much more prominent compared with nucleation particles, which is consistent with the observation in Ref. [40]. The nucleation mode particles are mainly generated from condensation and nucleation of gaseous semi-volatile components in the exhaust gas [62, 63]. High THC concentration after combustion tends to produce high nucleation mode particle concentrations in the cooled exhaust gas during the sampling and dilution process. Compared to 93#, 93#E10 with ethanol and lower aromatic contents can improve the oxidation in the locally rich regions (high combustion efficiency), restrict aromatic ring initiation [48] and decrease activation energy of soot oxidation [15], which is conducive to THC and PN emission reduction (especially for accumulation particles) under SI mode. However, plenty of researches have proved that ethanol-gasoline blends have the risk of increasing the proportion of nucleation particles under poor-mixed or low load conditions [16], which can also be supported by Fig. 14 (b). Therefore, the injection strategy and ethanol contents for gasoline should be chosen carefully for SI combustion.

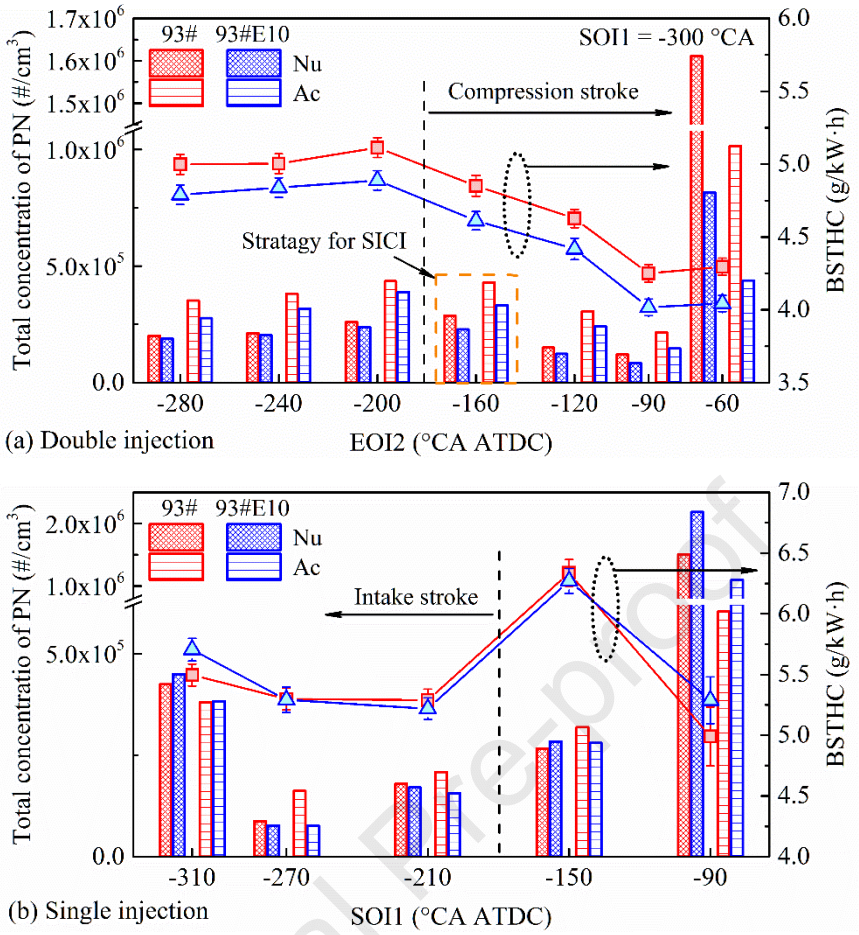

Fig. 14 Impact of ethanol blending on PN and THC under SI mode (1500 r/min, 0.5 MPa BMEP)

3.3.2 PN emissions of SICI under air dilution conditions

Fig. 15 shows the PN emission under SICI mode at the same engine load as Fig. 14. There are mainly three characteristics: (1) PN emission decreases with the increase of ethanol amount except for λ = 1.0 under high KI conditions; (2) for a given KI, the three fuels with ethanol content all have lower PN emission than 82# which has more aromatics and olefins; (3) blending ethanol can significantly decrease accumulation mode particles regardless of λ and the reduction degree increases as the mixture become leaner. The box charts in Fig. 15 (b), (d) and (f) show the distributions of PN when sweeping spark timing for each fuel, and the corresponding total concentration of PN at each spark timing is shown in Fig. 15 (a), (c) and (e), respectively.

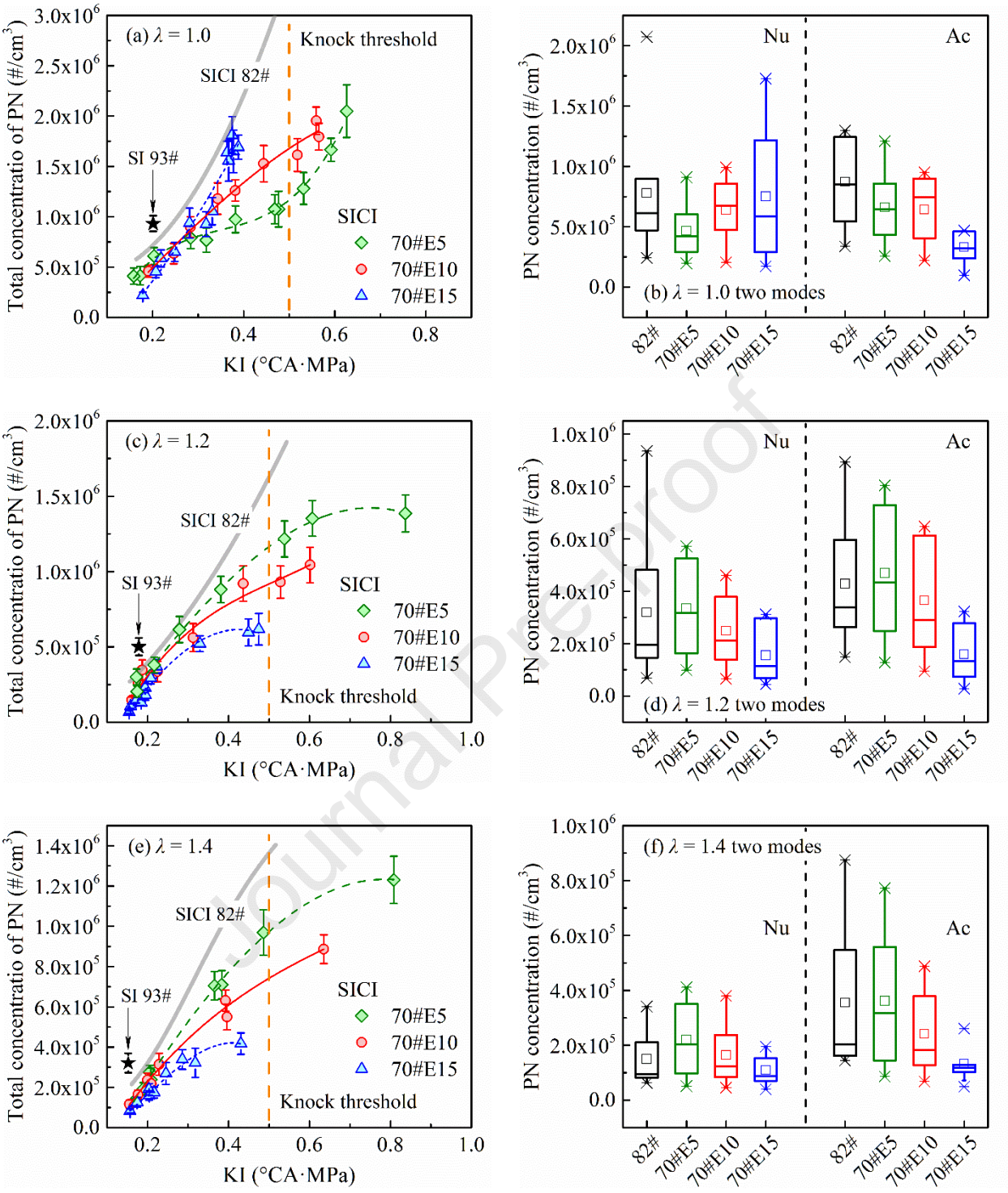

Fig. 15 PN emission of fuels with different ethanol contents under air dilution conditions. In a box chart, the cross represents the 1st and 99th percentile. The square and the short horizontal line of each box represent the average and median value, respectively. The box's range is from the 25th to 75th percentile.

The abnormal PN increase with ethanol amount under λ = 1.0 and high KI conditions is due to significant increase of nucleation mode particles caused by THC increase as shown in Fig. 16. The

THC increase can be attributed to two factors. Firstly, the effect of ethanol on THC oxidation during the flame propagation stage is weakened when the RON of base gasoline is reduced to 70# which has much lower aromatic contents. Secondly, ethanol performs chemical inertness under the current thermodynamic states, which restricts auto-ignition intensity and retards combustion phasing (Fig. 6), resulting in higher THC and nucleation mode particles during the compression ignition stage [12, 44, 56, 64]. Since 70#E15 has the most ethanol among the three ethanol-blended fuels, its THC will correspondingly deteriorate the most under high KI conditions, which finally exhibits the highest nucleation mode particles.

As the mixture becomes leaner, the rich-oxygenated and low-reactivity environment improves THC oxidation during the flame propagation stage and simultaneously restricts KI, and the difference in THC between the three ethanol-contained fuels becomes narrower. Even though the THC emission of 70#E15 is the highest and is not conducive to PN reduction, the total PN concentration of 70#E15 is the lowest especially for accumulation mode particles, as shown in Fig. 15 (d) and (f). To analyze the reason of accumulation particle reduction, previous results of particle emission in HCCI combustion can be referred to separate the influence of deflagration and auto-ignition portion in SICI. It has been reported that the accumulation mode particles under HCCI combustion are even more than SI mode when using direct injection under the similar load [49, 50]. In HCCI combustion using gasoline and low-carbon alcohols, accumulation mode particles are usually more than nucleation mode particles under various engine loads [45, 65, 66], and ethanol has no obvious advantage in reducing accumulation mode particle compared with pure gasoline [45]. Therefore, considering the results in Fig. 14-Fig. 16 and the aforementioned analysis, it can be inferred that decreased accumulation mode particles during flame propagation are the dominant

factor in reducing the total PN concentration in air-diluted SICI combustion.

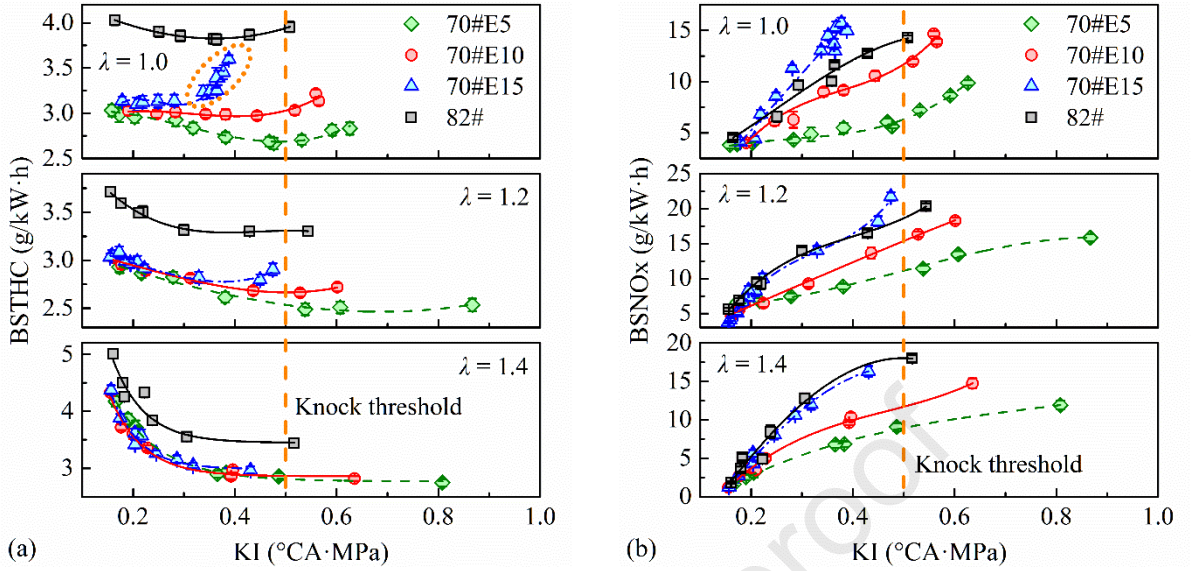

Fig. 16 THC and NO_x emissions under air dilution SICI combustion

The NO_x emission of 70#E5-E15 increases with ethanol content, indicating higher combustion temperature in the cylinder. Basically, it is difficult for 70#E15 which has high RON and S to achieve SICI mode unless more advanced ST is used to promote end-gas autoignition. Thus, low fuel consumption for 70#E15 can only be achieved at the cost of significant increase in NO_x and THC [25]. This trade-off relationship can be alleviated with lean burn because a higher temperature in lean mixture facilitates THC and soot oxidation during the late stage of combustion. Together with the low activation energy of oxidation for soot in ethanol-gasoline environment, the PN emission decreases as ethanol amount rises.

3.3.3 PN emissions of SICI under EGR conditions

The effects of ethanol on PN reduction under EGR conditions can be seen in Fig. 17 and Fig. 18. It should be noted that for the EGR rate more than 10%, the PN concentration of 70#E10 is higher than 70# due to the low dilution tolerance of ethanol, but it is still lower than 82#. The low dilution tolerance results in the poor combustion stability, shown as high coefficient of variation of IMEP (COV_{IMEP}). For example, COV_{IMEP} are 1.8%/1.3% (EGR = 15%) and 3.0%/1.6% (EGR = 20%) for

70#E10/82# respectively under MBT conditions of 2000 r/min and 0.8 MPa. High cycle-to-cycle fluctuation with 20% EGR could also be found in Fig. 6 (f), more dispersed distribution of 70#E10 compared with 82#. If the spark timing keeps the same under heavy diluted conditions, the difference in COV_{IMEP} between 70#E10 and 82# will be further enlarged. This means that PN emissions are simultaneously influenced by in-cylinder combustion process and fuel composition. When EGR is not more than 10%, the effect of ethanol addition is opposite to that of increasing aromatics and olefins (unsaturation) on PN emission. In contrast, with EGR over 10%, both blending ethanol and high aromatics/olefins amount increase PN, which could be attributed to the low combustion stability for ethanol-contained fuels. Whatever the EGR rate is, the degree of unsaturation is dominant, demonstrated as the highest PN for 82# among the three fuels. High unsaturation components can produce a large number of precursors of particles such as polycyclic aromatic hydrocarbons (PAHs) [67] which directly participate in the formation of particles. On the other hand, the maximum temperature drops with increasing EGR rate, which also suppresses thermal pyrolysis and dehydrogenation reaction of fuels [40] and is conducive to the total PN reduction.

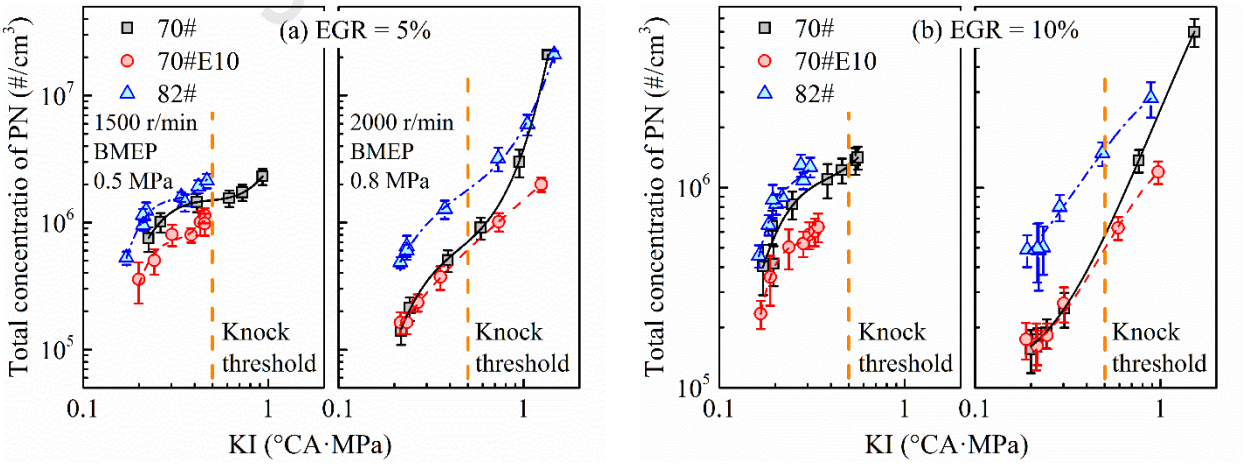

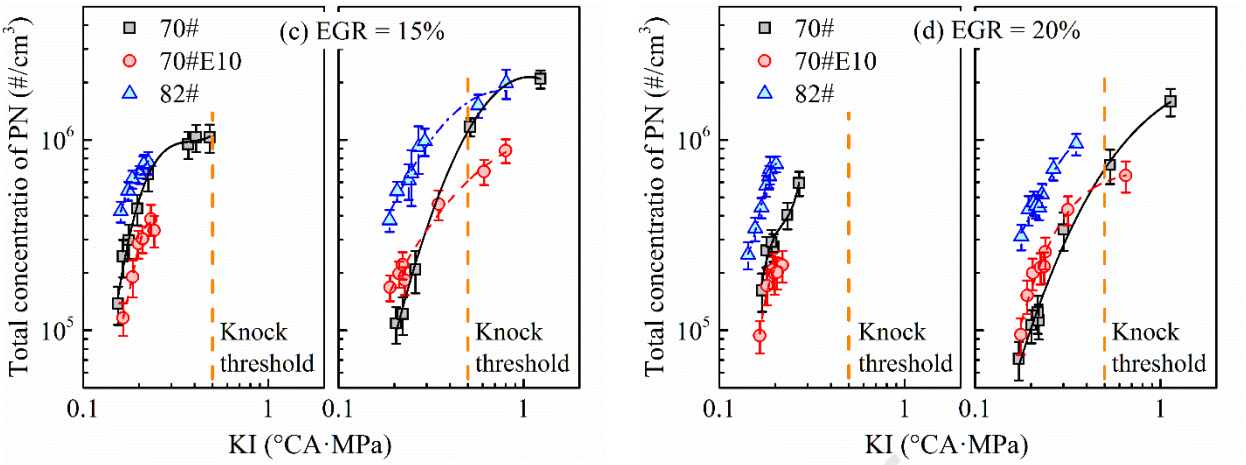

Fig. 17 PN emission under EGR conditions using fuels with different ethanol contents

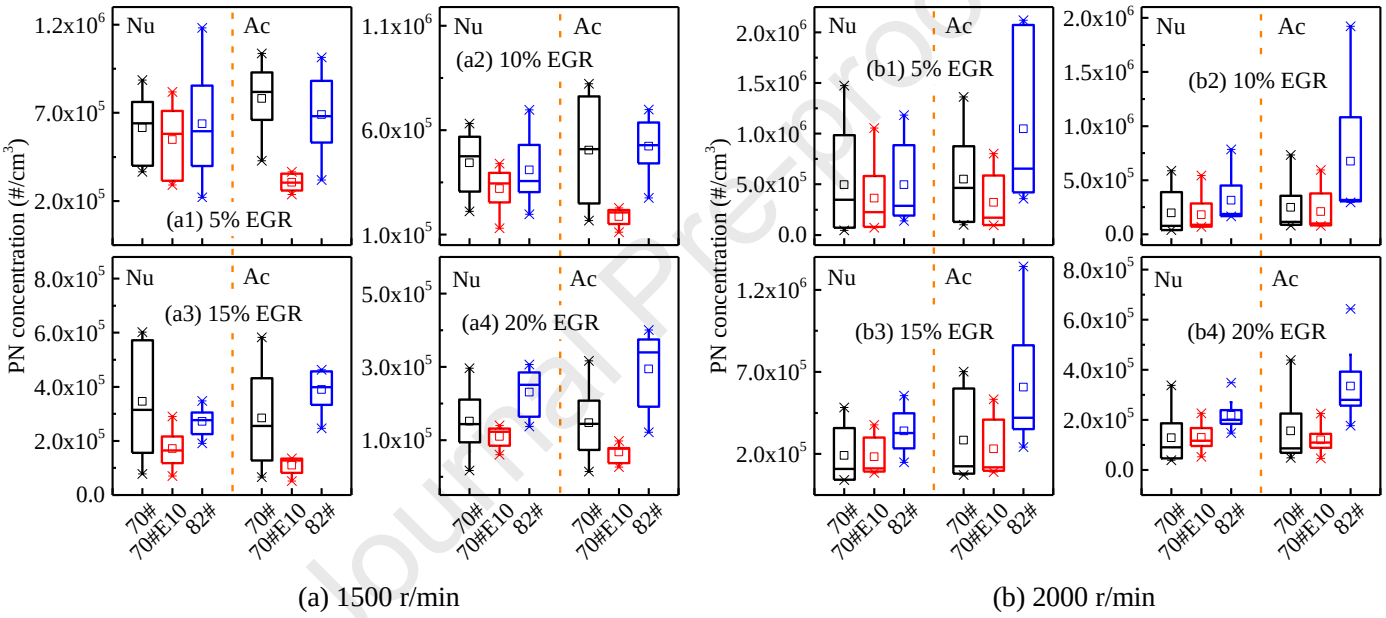

(a) 1500 r/min (b) 2000 r/min

Fig. 18 Comparison of nucleation and accumulation mode particles at different EGR rates. The cases with KI over 1.0 were not included due to high uncertainty

It can be well recognized from Fig. 18 that the accumulation mode particles of 70#E10 is much lower than 70# and 82#, which contributes to the lowest total PN concentration of 70#E10 among three fuels under most conditions. Similar to the cases under air dilution condition, the reduction of accumulation particles is mainly attributed to the high-*T* oxidation during the flame propagation stage. However, once the combustion stability is much decreased with EGR over 10% at 2000 r/min, the effect of flame propagation stage on reducing accumulation particle will be weakened, which is supported by the gradually ascending position of median line of 70#E10 in Fig. 18 compared with

70# with increasing EGR. Combustion instability also increases THC and combustion loss, as shown in Fig. 19 and Fig. 12 respectively.

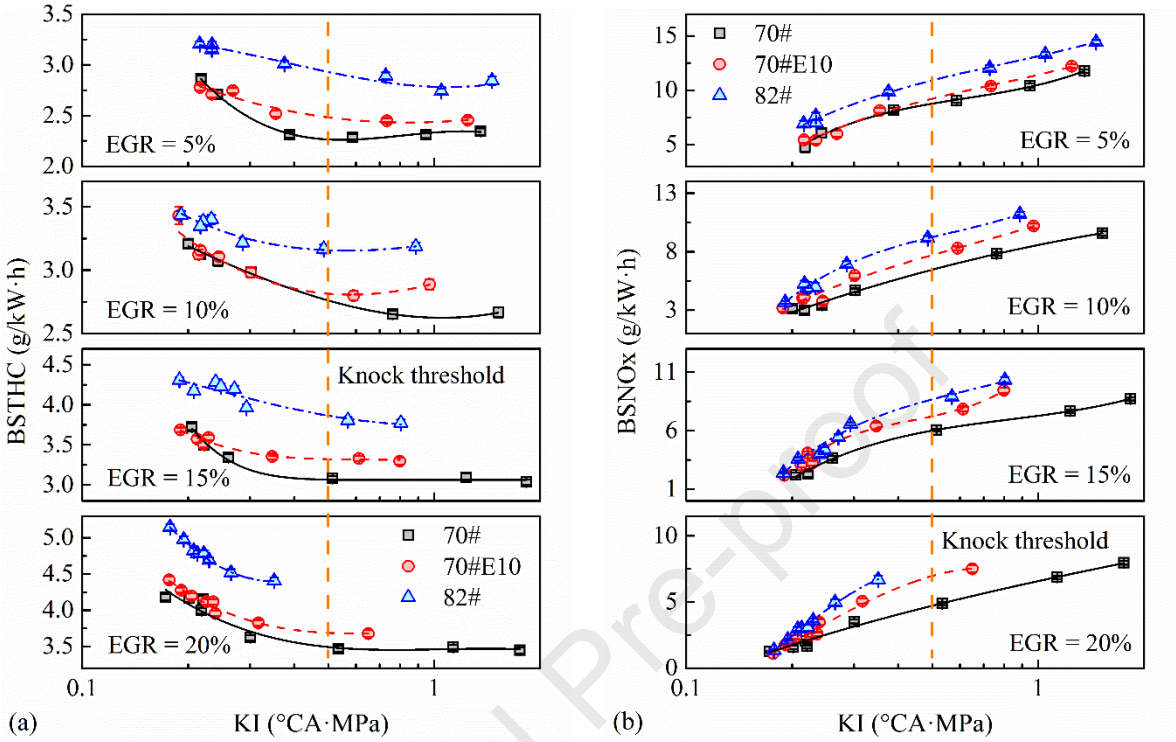

Fig. 19 Characteristic of gaseous emissions under EGR conditions (2000 r/min, 0.8 MPa BMEP)

Fig. 19 shows that under the conditions that produce higher PN for 70#E10 than 70#, the NOx of 70#E10 is also slightly higher than 70#. In other words, there is no trade-off between particle emission and NOx, and the increased PN is mainly caused by ethanol's low dilution tolerance rather than in-cylinder temperature. In addition, the performance that 82# always has the highest NO_x emission can interpret the PN's characteristic of 82#. The highest NO_x means the highest temperature during the late stage of combustion. Combining the influence of in-cylinder temperature with degree of unsaturation, it is reasonable that the higher unsaturation and higher rate of thermal pyrolysis generates more particles for 82# than for 70# and 70#E10 [46, 67]. In consequence, PN emissions of 82# are the worst among the three fuels.

3.4 Discussion on using ethanol better under SICI combustion

Based on the aforementioned analysis on combustion characteristics and PN emissions of SICI,

the anti-knock performance of ethanol results in incomplete compression ignition combustion and THC increase, which has a risk of deterioration in nucleation mode particles. Moreover, the low reactivity of ethanol due to the low thermodynamic states of TDC restricts the lean limit and EGR tolerance of engine operation and is not beneficial to combustion phasing adjustment and fuel economy improvement. Therefore, further enhancing chemical reactivity of ethanol-contained fuels is required for the lean or EGR diluted SICI combustion to better fulfill fuel-engine co-optima. Fig. 20 illustrates the *T-p* trajectories of 70#-70#E15 obtained on the current engine overlapped with ignition delay contours calculated using a reduced LLNL gasoline surrogate mechanism [68]. The "star" on each curve represents CA2, i.e., the initial thermal state at which the burned mass fraction reaches 2%. The temperature calculated at CA2 from the pressure history can represent the bulk gas temperature in the entire combustion chamber due to negligible heat release [69].

The light purple curve with circles (Curve 1) and light purple curve with triangles (Curve 2) are the demarcation curves of ethanol-isooctane reactivity at λ = 1.0 and λ = 2.0 respectively, extracted from our previous work [14, 36]. It is clear that the thermal states at CA2 of the four fuels are all to the left of Curve 1, which supports the conclusion in the above sections that ethanol performs chemical inertness and knock resistance currently. In order to further extend the lean burn limit, a higher CR and moderately intake heating are required to shorten the ignition delay of ethanol, so that the thermal state of bulk gas will move towards Curve 2. A combustion system with CR more than 15.0 and λ > 1.6 has the potential to achieve 750~800 K in cylinder near TDC at normal temperature and pressure [36]. Comparing the thermal state of Curve 1 with Curve 2, the H-extraction route for ethanol has changed from α-H to β-H [59] and the OH radical concentration increases rapidly, indicating an enhanced chemical reactivity of the reaction system. In this situation, ethanol-gasoline

blends can be fully taken advantage of on the reduction of fuel consumption and PN emissions.

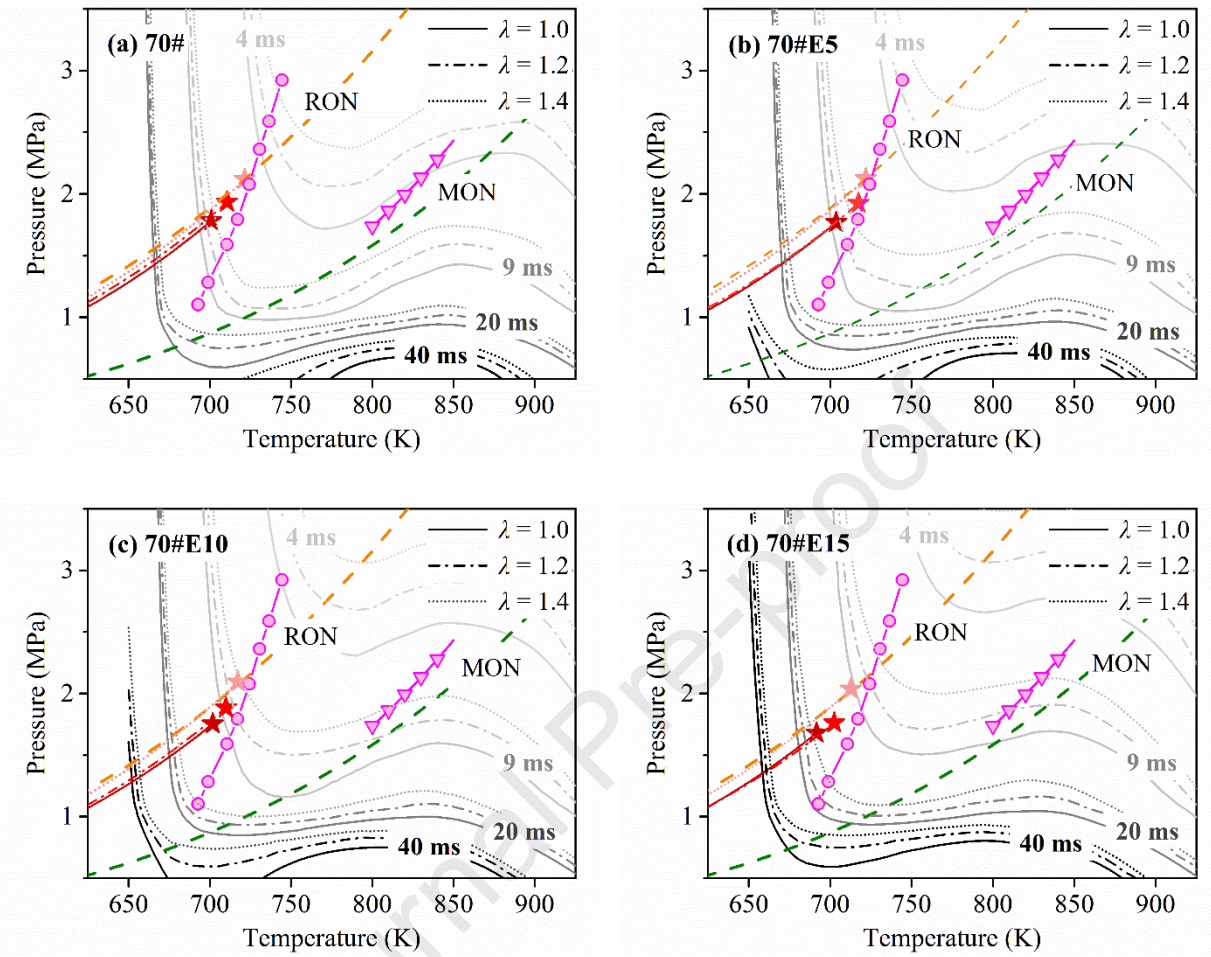

Fig. 20 *T-p* trajectory in the current engine under SICI combustion. The light purple-circle curves with circles and triangles respectively represent the demarcation curves of ethanol-isooctane reactivity at λ = 1.0 and λ = 2.0. The stars denote CA2 at MBT under 1500 r/min and 0.5 MPa BMEP

4. Conclusions

The objective of this study is to systematically investigate the influence of ethanol on SICI engine performance including combustion characteristic, fuel economy and PN emissions. To this end, SICI combustion fueled with different ethanol-gasoline blends was achieved under air dilution and EGR conditions in a mass-production engine with a CR of 12. The effect of blending ethanol on SICI was investigated in terms of combustion characteristics, fuel economy and PN emissions. The required optimization on engine's compression ratio and operating conditions for further improving

SICI performance were discussed based on *T-p* trajectories coupled with ignition delay contours. Some conclusions can be drawn as follows:

1. Ethanol addition into gasoline by splash blending exhibited anti-knock behavior, and the KI decreased with increasing ethanol content. The synergistic effect on auto-ignition between ethanol and aromatics could be found when comparing ethanol-gasoline blend to pure gasoline with the same RON. In this situation, the ethanol-gasoline blends showed higher fuel reactivity (larger KI), which could be identified in different engine operating conditions.
2. Ethanol-gasoline blend had a lower EGR tolerance in SICI combustion than pure gasoline especially during the stage of flame propagation, which would result in longer spark delay, later auto-ignition timing, decreased fuel economy and higher PN emissions under highly diluted conditions. In the situation with moderate EGR and air dilution, blending ethanol could advance CA50 to the optimal region, significantly decreasing the minimum $BSFC_{eq}$ compared with base gasolines and SI mode.
3. From the viewpoint of energy balance analysis, the ratio of heat transfer loss under SICI was more than 30% under both lean-burn and EGR conditions. Even though lean-burn could reduce exhaust loss, its longer combustion duration than stoichiometric condition would result in obviously more heat transfer loss. Therefore, to extend lean burn limit and improve thermal efficiency for SICI, a more reactive mixture and a shorter combustion duration will be required.
4. Considering CA50 could not comprehensively reflect fuel economy of SICI combustion, two dimensionless parameters, AHRA/FBHR and (CA90-CA50)/(CA50-CA10) were defined . These two parameters extracted from the cycles with high thermal efficiency could be well correlated in the form of exponential fitting, showing fuel independence.

5. Generally, blending ethanol could reduce PN emissions in SICI combustion except for the cases with high KI at λ = 1.0 and the cases with poor combustion quality under high EGR ratio conditions where nucleation mode particles increased significantly. Total PN reduction was mainly due to the decrease of accumulation mode particles, which was primarily attributed to temperature rise in the stage of flame propagation. For a fixed KI, adding ethanol to pure gasoline would increase THC and NOx emissions due to the lowered auto-ignition tendency and more advanced combustion phasing requirement to keep combustion stable. Therefore, further increasing CR along with slight intake heating to improve the reactivity of the air-fuel mixture is the next step to achieve better fuel economy and PN emission for diluted SICI combustion.

Acknowledgments

This work was supported by the National Key Research and Development Program of China (Grant No. 2017YFE0102800) and the National Natural Science Foundation of China (Grant No. 52076118). The assistance of Dr. Haoye Liu at the University of Birmingham in paper writing and language improvement was also gratefully acknowledged.

Reference

[1] Wang Z, He X, Wang J-X, Shuai S, Xu F, Yang D. Combustion visualization and experimental study on spark induced compression ignition (SICI) in gasoline HCCI engines. Energy Conversion and Management, 2010, 51(5): 908-17.

[2] Xie H, Li L, Chen T, Yu W, Wang X, Zhao H. Study on spark assisted compression ignition (SACI) combustion with positive valve overlap at medium–high load. Applied Energy, 2013, 101: 622-33.

[3] Olesky LM, Martz JB, Lavoie GA, Vavra J, Assanis DN, Babajimopoulos A. The effects of spark timing, unburned gas temperature, and negative valve overlap on the rates of stoichiometric spark assisted compression ignition combustion. Applied Energy, 2013, 105: 407-17.

[4] Ortiz-Soto EA, Lavoie GA, Martz JB, Wooldridge MS, Assanis DN. Enhanced heat release analysis for advanced multi-mode combustion engine experiments. Applied Energy, 2014, 136: 465-79.

[5] Olesky LKM, Middleton RJ, Lavoie GA, Wooldridge MS, Martz JB. On the sensitivity of low temperature combustion to spark assist near flame limit conditions. Fuel, 2015, 158: 11-22.

[6] Zhou L, Hua J, Wei H, Dong K, Feng D, Shu G. Knock characteristics and combustion regime diagrams of multiple combustion modes based on experimental investigations. Applied Energy, 2018, 229: 31-41.

[7] Nakai E, Goto T, Ezumi K, Ezumi K, Tsumura Y, Endou K, Kanda Y, et al. MAZDA SKYACTIV-X 2.0L Gasoline Engine. 28th Aachen Colloquium Automobile and Engine Technology. 2019:55-78.

[8] Kalghatgi G, Levinsky H, Colket M. Future transportation fuels. Progress in Energy and Combustion Science, 2018, 69: 103-5.

[9] Sari RL, Golke D, Enzweiler HJ, Salau NPG, Pereira FM, Martins MES. Exploring optimal operating conditions for wet ethanol use in spark ignition engines. Applied Thermal Engineering, 2018;138:523–33.

[10] Wang C, Zeraati-Rezaei S, Xiang L, Xu H. Ethanol blends in spark ignition engines: RON, octane-added value, cooling effect, compression ratio, and potential engine efficiency gain. Applied Energy, 2017, 191: 603-19.

[11] Dong S, Wang Z, Yang C, Ou B, Lu H, Xu H, et al. Investigations on the effects of fuel stratification on auto-ignition and combustion process of an ethanol/diesel dualfuel engine. Applied Energy, 2018;230:19–30.

[12] Belgiorno G, Di Blasio G, Shamun S, Beatrice C, Tunestål P, Tunér M. Performance and emissions of diesel-gasoline-ethanol blends in a light duty compression ignition engine. Fuel, 2018, 217: 78-90.

[13] Szybist JP, Splitter DA. Pressure and temperature effects on fuels with varying octane sensitivity at high load in SI engines. Combustion and Flame, 2017, 177: 49-66.

[14] Fan Q, Wang Z, Qi Y, Wang Y. Investigating auto-ignition behavior of n-heptane/iso-octane/ethanol mixtures for gasoline surrogates through rapid compression machine measurement and chemical kinetics analysis. Fuel, 2019, 241: 1095-108.

[15] Luo Y, Zhu L, Fang J, Zhuang Z, Guan C, Xia C, et al. Size distribution, chemical composition and oxidation reactivity of particulate matter from gasoline direct injection (GDI) engine fueled with ethanol-gasoline fuel. Applied Thermal Engineering, 2015, 89: 647-55.

[16] Wang C, Xu H, Herreros JM, Wang J, Cracknell R. Impact of fuel and injection system on particle emissions from a GDI engine. Applied Energy, 2014, 132: 178-91.

[17] Wang Z, Liu H, Reitz RD. Knocking combustion in spark-ignition engines. Progress in Energy and Combustion Science, 2017, 61: 78-112.

[18] Han T, Singh R, Lavoie G, Wooldridge M, Boehman A. Multiple injection for improving knock, gaseous and particulate matter emissions in direct injection SI engines. Applied Energy, 2020, 262: 114578.

[19] Gong C, Zhang Z, Sun J, Chen Y, Liu F. Computational study of nozzle spray-line distribution effects on stratified mixture formation, combustion and emissions of a high compression ratio DISI methanol engine under lean-burn condition. Energy, 2020, 205: 118080.

[20] Wang Z, Liu H, Long Y, Wang J, He X. Comparative study on alcohols–gasoline and gasoline–alcohols dual-fuel spark ignition (DFSI) combustion for high load extension and high fuel efficiency. Energy, 2015, 82: 395-405.

[21] Liu H, Wang Z, Long Y, Xiang S, Wang J, Wagnon SW. Methanol-gasoline Dual-fuel Spark Ignition (DFSI) combustion with dual-injection for engine particle number (PN) reduction and fuel economy improvement. Energy, 2015, 89: 1010-1017.

[22] Gong C, Li Z, Sun J, Liu F. Evaluation on combustion and lean-burn limit of a medium compression ratio hydrogen/methanol dual-injection spark-ignition engine under methanol late-injection. Applied Energy, 2020, 277: 115622.

[23] Gong C, Li Z, Yi L, Liu F. Experimental investigation of equivalence ratio effects on combustion and emissions characteristics of an H2/methanol dual-injection engine under different spark timings. Fuel, 2020, 262: 116463.

[24] Sjöberg M, Zeng W. Combined Effects of Fuel and Dilution Type on Efficiency Gains of Lean Well-Mixed DISI Engine Operation with Enhanced Ignition and Intake Heating for Enabling Mixed-Mode Combustion. SAE International Journal of Engines, 2016, 9(2): 750-67.

[25] D.F. Chuahy F, Powell T, Curran SJ, Szybist JP. Impact of fuel chemical function characteristics on spark assisted and kinetically controlled compression ignition performance focused on multi-mode operation. Fuel,

2021, 299: 120844.

[26] Olesky LM, Lavoie GA, Assanis DN, Wooldridge MS, Martz JB. The effects of diluent composition on the rates of HCCI and spark assisted compression ignition combustion. Applied Energy, 2014, 124: 186-98.

[27] Chen L, Zhang R, Pan J, Wei H. Effects of partitioned fuel distribution on auto-ignition and knocking under spark assisted compression ignition conditions. Applied Energy, 2020, 260: 114269.

[28] Zhou L, Song Y, Hua J, Liu F, Wei H. Effects of miller cycle strategies on combustion characteristics and knock resistance in a spark assisted compression ignition (SACI) engine. Energy, 2020, 206: 118119.

[29] Hunicz J, Mikulski M, Koszałka G, Ignaciuk P. Detailed analysis of combustion stability in a spark-assisted compression ignition engine under nearly stoichiometric and heavy EGR condition. Applied Energy, 2020, 280: 115955.

[30] Gentz G, Dernotte J, Ji C, and Dec J. Spark Assist for CA50 Control and Improved Robustness in a Premixed LTGC Engine Effects of Equivalence Ratio and Intake Boost. SAE Technical Paper 2018-01-1252, 2018.

[31] Hu Z, Zhang J, Sjöberg M, Zeng W. The use of partial fuel stratification to enable stable ultra-lean deflagration-based Spark-Ignition engine operation with controlled end-gas autoignition of gasoline and E85. International Journal of Engine Research, 2020, 21(9): 1678-95.

[32] Qi Y, Wang Z, Wang J, He X. Effects of thermodynamic conditions on the end gas combustion mode associated with engine knock. Combustion and Flame, 2015;162(11):4119–28.

[33] Pan J, Hu Z, Wei H, Pan M, Liang X, Shu G, et al. Understanding strong knocking mechanism through high-strength optical rapid compression machines. Combustion and Flame, 2019, 202: 1-15.

[34] Strozzi C, Claverie A, Prevost V, Sotton J, Bellenoue M. HCCI and SICI combustion modes analysis with simultaneous PLIF imaging of formaldehyde and high-speed chemiluminescence in a rapid compression machine. Combustion and Flame, 2019, 202: 58-77.

[35] Assanis D, Wagnon SW, Wooldridge MS. An experimental study of flame and autoignition interactions of iso-octane and air mixtures. Combustion and Flame, 2015, 162(4): 1214-24.

[36] Fan Q, Qi Y, Wang Z. Impact of octane sensitivity and thermodynamic conditions on combustion process of spark-ignition to compression-ignition through an optical rapid compression machine. Fuel, 2019, 253: 864-80.

[37] Fan Q, Qi Y, Wang Z. Effect of octane number and thermodynamic conditions on combustion process of spark ignition to compression ignition through a rapid compression machine. Fuel, 2020, 262: 116480.

[38] Urushihara T, Yamaguchi K, Yoshizawa K, Itoh T. A Study of a Gasoline-fueled Compression Ignition Engine ～ Expansion of HCCI Operation Range Using SI Combustion as a Trigger of Compression Ignition ～. SAE technical paper 2005-01-0180, 2005.

[39] Mendrea B, Chang Y, Akkus YZA, Sterniak J, Bohac S. Investigations of the Effect of Ambient Condition on SACI Combustion Range. SAE Technical Paper 2015-01-0828, 2015.

[40] Zhang Z, Wang T, Jia M, Wei Q, Meng X, Shu G. Combustion and particle number emissions of a direct injection spark ignition engine operating on ethanol/gasoline and n-butanol/gasoline blends with exhaust gas recirculation. Fuel, 2014, 130: 177-88.

[41] Cho J, Si W, Jang W, Jin D, Myung C-L, Park S. Impact of intermediate ethanol blends on particulate matter emission from a spark ignition direct injection (SIDI) engine. Applied Energy, 2015, 160: 592-602.

[42] Wu X, Zhang S, Guo X, Yang Z, Liu J, He L, et al. Assessment of ethanol blended fuels for gasoline vehicles in China: Fuel economy, regulated gaseous pollutants and particulate matter. Environmental Pollution, 2019, 253: 731-40.

[43] Belgiorno G, Di Blasio G, Shamun S, Beatrice C, Tunestål P, Tunér M. Performance and emissions of diesel-gasoline-ethanol blends in a light duty compression ignition engine. Fuel, 2018, 217: 78-90.

[44] Pachiannan T, Zhong W, Rajkumar S, He Z, Leng X, Wang Q. A literature review of fuel effects on performance and emission characteristics of low-temperature combustion strategies. Applied Energy, 2019, 251: 113380.

[45] Maurya RK, Agarwal AK. Experimental investigations of particulate size and number distribution in an ethanol and methanol fueled HCCI engine. Journal of Energy Resources Technology, Transactions of the ASME, 2015, 137(1).

[46] Qian Y, Li Z, Yu L, Wang X, Lu X. Review of the state-of-the-art of particulate matter emissions from modern gasoline fueled engines. Applied Energy, 2019, 238: 1269-98.

[47] Bogarra M, Herreros JM, Tsolakis A, Rodríguez-Fernández J, York APE, Millington PJ. Gasoline direct injection engine soot oxidation: Fundamentals and determination of kinetic parameters. Combustion and Flame, 2018, 190: 177-87.

[48] Sementa P, Maria Vaglieco B, Catapano F. Thermodynamic and optical characterizations of a high performance GDI engine operating in homogeneous and stratified charge mixture conditions fueled with gasoline and bio-ethanol. Fuel, 2012, 96: 204-19.

[49] Kaiser EW, Yang J, Culp T, Xu N, Maricq MM. Homogeneous charge compression ignition engine-out emission-does flame propagation occur in homogeneous charge compression ignition?. International Journal of Engine Research, 2002, 3(4): 185-95.

[50] Price P, Stone R, Misztal J, Xu H, Wyszynski M, Wilson T, et al. Particulate emissions from a gasoline homogeneous charge compression ignition engine. SAE Technical Papers 2007-01-0209, 2007.

[51] Fan Q, Wang Z, Qi Y, Liu S, Sun X. Research on ethanol and toluene's synergistic effects on auto-ignition and pressure dependences of flame speed for gasoline surrogates. Combustion and Flame, 2020, 222: 196-212.

[52] Wang C, Janssen A, Prakash A, Cracknell R, Xu H. Splash blended ethanol in a spark ignition engine – Effect of RON, octane sensitivity and charge cooling. Fuel, 2017, 196: 21-31.

[53] Foong TM, Morganti KJ, Brear MJ, da Silva G, Yang Y, Dryer FL. The octane numbers of ethanol blended with gasoline and its surrogates[J]. Fuel, 2014, 115: 727-39.

[54] Lipatnikov AN. Stratified turbulent flames: Recent advances in understanding the influence of mixture inhomogeneities on premixed combustion and modeling challenges. Progress in Energy and Combustion Science, 2017, 62: 87-132.

[55] Andreae M, Cheng W, Kenney T, and Yang J. On HCCI Engine Knock. SAE Technical Paper 2007-01-1858, 2007.

[56] Yu L, Shuai S, Li Y, Li B, Liu H, He X, et al. An experimental investigation on thermal efficiency of a compression ignition engine fueled with five gasoline-like fuels. Fuel, 2017, 207: 56-63.

[57] Li B, Li Y, Liu H, Liu F, Wang Z, Wang J. Combustion and emission characteristics of diesel engine fueled with biodiesel/PODE blends[J]. Applied Energy, 2017, 206: 425-31.

[58] Fan Q, Qi Y, Wang Y, Wang Z. Investigation into pressure dependence of flame speed for fuels with low and high octane sensitivity through blending ethanol. Combustion and Flame, 2020, 212: 252-69.

[59] Lu Z, Yang Y, Brear MJ. Impact of ethanol on oxidation of iso-octane at low and intermediate temperatures. Combustion and Flame, 2020, 214: 167-83.

[60] Lee C, Ahmed A, Nasir EF, Badra J, Kalghatgi G, Sarathy SM, et al. Autoignition characteristics of oxygenated gasolines. Combustion and Flame, 2017, 186: 114-28.

[61] Robertson D, Prucka R. Evaluation of autoignition models for production control of a spark-assisted compression ignition engine. International Journal of Engine Research, 2020.

[62] Liu H, Li Z, Xu H, Ma X, Shuai S. Nucleation mode particle evolution in a gasoline direct injection engine with/without a three-way catalyst converter. Applied Energy, 2020, 259: 114211.

[63] Pirjola L, Karl M, Rönkkö T, Arnold F. Model studies of volatile diesel exhaust particle formation: are organic vapours involved in nucleation and growth? Atmospheric Chemistry And Physics, 2015, 15(18): 10435-52.

[64] Fang Q, Fang J, Zhuang J, Huang Z. Effects of ethanol–diesel–biodiesel blends on combustion and emissions in premixed low temperature combustion. Applied Thermal Engineering, 2013, 54(2): 541-8.

[65] Maurya RK, Agarwal AK. Effect of intake air temperature and air-fuel ratio on particulates in gasoline and n-butanol fueled homogeneous charge compression ignition engine. International Journal of Engine Research, 2014, 15(7): 789-804.

[66] Agarwal AK, Gupta T, Lukose J, Singh AP. Particulate Characterization and Size Distribution in the Exhaust of a Gasoline Homogeneous Charge Compression Ignition Engine. Aerosol and Air Quality Research, 2015, 15(2): 504-16.

[67] Zhao F, Yang W, Yu W, Li H, Sim YY, Liu T, et al. Numerical study of soot particles from low temperature combustion of engine fueled with diesel fuel and unsaturation biodiesel fuels. Applied Energy, 2018, 211: 187-93.

[68] Mechanism https://combustion.llnl.gov/mechanisms/surrogates/gasolinesurrogate.

[69] Splitter DA, Gilliam A, Szybist J, Ghandhi J. Effects of pre-spark heat release on engine knock limit. Proceedings of the Combustion Institute, 2019, 37(4): 4893-900.

HIGHLIGHTS

- Ethanol's effects under spark-ignition to compression-ignition mode is investigated
- Synergistic effect between ethanol and aromatics on auto-ignition was verified
- Two dimensionless parameters are proposed to characterize high-efficiency cycles
- Accumulation mode particles are lowered during flame propagation rather than auto-ignition

Declaration of interests

☒ The authors declare that they have no known competing financial interests or personal relationships that could have appeared to influence the work reported in this paper.

☐The authors declare the following financial interests/personal relationships which may be considered as potential competing interests: